From the Department of Ophthalmology
Saarland University Medical Center, Homburg/Saar
(Chairman: Professor Dr. B. Seitz)

Effect of phacoemulsification on the corneal biomechanical properties

–

Auswirkungen der Phakoemulsifikation auf biomechanische Eigenschaften der Hornhaut

Dissertation for the degree of Doctor in Medicine
Faculty of Medicine
UNIVERSITY OF SAARLAND

2016

Presented by
Moatasem El-Husseiny
Born on 28.09.1973 in Tubruk, Libya

Tag der Promotion:

Dekan:

1. Berichterstatter:

2. Berichterstatter:

TABLE OF CONTENTS

LIST OF ABBREVIATIONS:

AL	Axial length
CCI	Clear corneal incision
CCT	Central corneal thickness
CH	Corneal Hystereses
CRF	Corneal resistance factor
CSI	Center surround index
CYL_{aCASIA}	Casia anterior cylinder power
CYL_{AR}	Autorefraktor cylinder equivalent power
CYL_{IOL}	IOL Master cylinder equivalent power
CYL_{pCASIA}	Casia posterior cylinder power
CYL_{TMS}	TMS cylinder power
DPT	Diopters
DSI	Differential sector index
ECC	Endothelial cell count
EQ_{aCASIA}	Casia anterior equivalent power
EQ_{AR}	Autorefractor anterior equivalent power
EQ_{IOL}	IOL Master anterior equivalent power
EQ_{pCASIA}	Casia posterior equivalent power
EQ_{TMS}	TMS anterior equivalent power
FHWM	Full Width at Half Maximum

IOL	Intraocular lens
IOPcc	Corneal compensated intraocular pressure
IOPg	Goldmann-related intraocular pressure
OCT	Ocular Coherence Tomography
ORA	Ocular Response Analyzer
OSI	Opposite sector index
OVD	Ophthalmic Viscosurgical Device
P1/P2	Peaks of the applanation curves of the Ocular response analyzer
SAI	Surface asymmetry index
SD	Standard deviation

SUMMARY

1.1 Zusammenfassung

1.1.1 Hintergrund

Der geübte Kataraktchirurg plant minutiös operative Manipulationen an der Hornhaut, da er weiß, dass Veränderungen der Biomechanik derselben durch clear cornea Zugang auch zu einer Änderung der refraktiven Parameter führen. Im ungünstigen Fall bewirken diese refraktiven Veränderungen eine Veränderung des intendierten postoperativen Ergebnisses. Teilweise vermag der Kataraktchirurg jedoch auch diese Veränderungen zu nutzen und sie in seine Operationsplanung mit einzubeziehen. Hierzu ist es jedoch notwendig, diese noch besser zu verstehen. In den vergangenen Jahren wurde zur besseren Untersuchung der biomechanischen Eigenschaften der Hornhaut der Ocular Response Analyzer (ORA) entwickelt. Die viskoelastischen Eigenschaften der Hornhaut haben einen nachweislichen Einfluss auf die Augeninnendruckmessung. Dieser Einfluss ist jedoch bislang nur bezüglich der Hornhautdicke untersucht. Es ist somit bislang unklar, wie der Augeninnendruck durch rein biomechanische Veränderungen beeinflusst wird. Ziel dieser Arbeit ist es, die mit dem ORA gemessenen biomechanischen Veränderungen der Hornhaut in Beziehung zu Standardparametern der ophthalmologischen Diagnostik vor und nach einfacher Phakoemulsifikation zu setzen.

1.1.2 Patienten und Methoden

In diese Studie wurden 54 Augen von 54 Patienten eingeschlossen. Alle Patienten hatten eine Linsentrübung im Stadium I oder II. Bei allen Patienten wurde der gleiche clear cornea Zugang gewählt. Die Patienten wurden präoperativ und 4 Wochen postoperativ zwischen 7 und 10 Uhr morgens untersucht, um eine Beeinflussung durch Tagesfluktuation zu vermeiden. Dabei wurden mit dem ORA folgende Zielgrößen bestimmt: Corneale Hysterese (CH), corneal resistance factor (CRF), Goldmann-related intraocular pressure (IOPg) und corneal compensated intraocular pressure (IOPcc). Analog wurden Untersuchungen mit dem Hornhauttopographiegerät TMS-5, dem Vorderabschnitts-OCT von CASIA, dem IOL-Master von Zeiss, dem Autorefraktor von Nidek, und dem EM-3000 von Tomey

durchgeführt. Hierbei wurden folgende Parameter bestimmt: anterior equivalent power (EQ_{TMS}), cylinder power (CYL_{TMS}), center surround index (CSI) und surface asymmetry index (SAI)); Casia anterior und posterior equivalent power (EQ_{aCASIA}, EQ_{pCASIA}) sowie Casia cylinder power (CYL_{aCASIA}, CYL_{pCASIA}). Mit dem IOL-Master wurden anterior equivalent power (EQ_{IOL}) und cylinder equivalent power (CYL_{IOL}) und Bulbuslänge (AL) untersucht; ebenso die entsprechenden Werte anterior equivalent power (EQ_{AR}) und cylinder equivalent power (CYL_{AR}) mit dem Autorefraktor. Mit dem EM-3000 wurden zentrale Hornhautdicke (CCT) und Endothelcellcount (ECC) extrahiert. Die Ergebnisse der ORA-Untersuchung wurden mittels Pearson-Korrelation mit denen der topograpischen Untersuchungen in Bezug gesetzt. Darüber hinaus wurde der Einfluss der präoperativen biometrischen Parameter auf die Änderung (Δ) der biomechanischen Zielgrößen untersucht.

1.1.3 Ergebnisse

Vor der Operation korrelierte die corneale Hysterese CH mit CYL_{TMS} (p=0,031), mit den Messergebnissen des Vorderabschnitts-OCTS EQ_{aCASIA} (p=0,033), CYL_{aCASIA} (p=0,04), EQ_{pCASIA} (p=0,001) und CYL_{pCASIA} (p=0,002), postoperativ mit EQ_{TMS} (p=0.038), EQ_{AR} (p=0,043), EQ_{aCASIA} (p=0,021) und EQ_{pCASIA} (p=0,022). Postoperativ korrelierten darüber hinaus IOPg und IOPcc mit allen gemessenen Brechkraftwerten (EQ_{TMS}, EQ_{IOL}, EQ_{AR}, EQ_{aCASIA} und EQ_{pCASIA}) (p=0,001, p=0,015, p=0,030, p=0,007, p=0,001 für IOPg und p<0,001, p=0,009, p=0,014, p=0,003, p<0,001 für IOPcc). Die durchschnittlichen Werte der Änderungen betrugen für ΔCH = -0,45±1,27 mmHg, ΔCRF = -0,88±1,1 mmHg, ΔIOPg = -1,58±3,15 mmHg und ΔIOPcc = -1,45±3,93 mmHg. Je höher CSI war, desto geringer war die Abnahme der CH (r = 0,302, p = 0,028). Je höher die CCT, desto größer war die Abnahme des CRF (r = -0,371, p = 0,013). Je höher die AL, desto geringer fiel die Abnahme des IOPg aus (r = 0,417, p = 0,005). Je höher AL, SAI und EEC, desto geringer war die Abnahme des IOPcc (r = 0,351, p = 0,001; r = -0,478, p < 0,001; r = 0,339, p = 0,013).

1.1.4 Schlussfolgerungen

Nach unseren Ergebnissen ist eine präoperativ flachere Hornhautrückfläche mit einer höheren cornealen Hystere assoziiert. Darüber hinaus sind eine postoperativ steilere Hornhautvorderfläche und eine flachere Hornhautrückfläche mit einer höheren

cornealen Hysterese assoziiert. Gleichzeitig sind steile Hornhautvorder- und-rückflächen mit einem höheren Augeninnendruck assoziiert. Dies bedeutet für den Kataraktpatienten, dass Informationen über die Brechkraft der Hornhautrückfläche dabei helfen können, die durch ORA bestimmten Werte (CH und IOPcc) korrekt einzuordnen. Die Änderung von biomechanischen Eigenschaften durch die Kataraktchirurgie wird von präoperativen biometrischen Parametern, wie z.B. Hornhautdicke und Augenlänge, signifikant beeinflusst. Ein Kataraktchirurg sollte vom biomechanischen Gesichtspunkt aus, sich nicht nur auf tomographische Untersuchungen verlassen, sondern auch den hornhautkompensierten Intraokulardruck, besonders für die Nachsorgeuntersuchungen nach Kataraktoperation berücksichtigen.

1.2 Summary

1.2.1 Background

Knowing that clear corneal incisions may lead to a change in the corneal biomechanics as well as the corneal refractive parameters, an experienced cataract surgeon always plans every corneal manipulation methodically. In critical cases, these refractive changes may cause alternate unintended postoperative results. However, the experienced cataract surgeon will consider these changes carefully and will plan his/her surgery accordingly. Thus, it is necessary to understand these changes. In recent years, it became possible to examine corneal biomechanics through the development of the Ocular Response Analyzer (ORA). It is well known, that the viscoelastic properties of the cornea play an important role in the applanation tonometry during the intraocular pressure (IOP) measurement. However, until today the focus has always been limited to a correlation between the IOP and corneal thickness. The influence of the corneal biomechanical changes on the IOP is unclear. The objective of our study is to investigate the correlation between the examined corneal biomechanical changes measured by the ORA, and the standard comprehensive ophthalmic examinations, before and after uneventful cataract phacoemulsification.

1.2.2 Patients and Methods

This study involved 54 eyes from 54 patients. All patients suffered from cataract with significant lens opacification in stages I or II. They underwent phacoemulsification with a clear corneal incision (2.8 mm incision). Each patient was examined before their intervention as well as 4 weeks after, between 7 and 10 a.m., to avoid the diurnal fluctuation. ORA was used to measure corneal hysteresis (CH), corneal resistance factor (CRF), Goldmann-related intraocular pressure (IOPg), and corneal compensated intraocular pressure (IOPcc). Concurrently, examinations from the corneal topography TMS-5, Casia anterior segment OCT, Zeiss IOL-Master, Nidek autorefractometer, and the Tomey EM-3000 were carried out. The biometric characteristics included: TMS-5 anterior equivalent power (EQ_{TMS}), cylinder (CYL_{TMS}) power, center surround index (CSI) and surface asymmetry index (SAI); Casia anterior and posterior equivalent (EQ_{aCASIA}, EQ_{pCASIA}) and cylinder (anterior and

posterior cylinder (CYL_{aCASIA}, CYL_{pCASIA}) power). Those parameters derived from the IOL-Master were anterior equivalent (EQ_{IOL}), cylinder (CYL_{IOL}) power and axial length (AL). In addition, the readings from the autorefractor were anterior equivalent (EQ_{AR}) and cylinder (CYL_{AR}) power. Central corneal thickness (CCT) and endothelial cell count (ECC) were extracted from the Tomey EM-3000. Results from ORA were analyzed using the Pearson Correlation method and compared with those from all other examinations. In addition, the impact of the preoperative biometric parameters, or the change (Δ) of biomechanical outcome measures, was investigated.

1.2.3 Results

During preoperative examination the corneal hysteresis (CH) was correlated with CYL_{TMS} (p=0.031), also with anterior segment OCT EQ_{aCASIA} (p=0.033), CYL_{aCASIA} (p=0.04), EQ_{pCASIA} (p=0.001) and CYL_{pCASIA} (p=0.002). During postoperative examination CH was correlated with EQ_{TMS} (p=0.038), EQ_{AR} (p=0.043), EQ_{aCASIA} (p=0.021) and EQ_{pCASIA} (p=0.022). Postoperatively, both the IOPcc and IOPg were correlated with all measured equivalent powers (EQ_{TMS}, EQ_{IOL}, EQ_{AR}, EQ_{aCASIA} and EQ_{pCASIA}) (p=0.001, p=0.015, p=0.030, p=0.007, p=0.001 for IOPg and p<0.001, p=0.009, p=0.014, p=0.003, p<0.001 for IOPcc). The average values of the changes of the biomechanical outcome measures were as follows: ΔCH = -0.45±1.27 mmHg, ΔCRF = -0.88±1.1 mmHg, ΔIOPg = -1.58±3.15 mmHg and ΔIOPcc = -1.45±3.93 mmHg. The higher CSI, the smaller the decrease in CH was (r = 0.302, p = 0.028). The higher CCT, the larger the decrease in CRF was (r = -0.371, p = 0.013). The higher AL, the smaller the decrease in IOPg was (r = 0.417, p = 0.005). The higher AL, SAI and ECC, the smaller the decrease in IOPcc was (r = 0.351, p = 0.001; r = -0.478, p < 0.001; r = 0.339, p = 0.013).

1.2.4 Conclusions

According to our results, a flatter corneal back surface before surgery is associated with a higher corneal hysteresis, while postoperatively a steeper corneal front surface and a flatter corneal back surface are associated with a higher corneal hysteresis. In addition, the steep corneal front and back surfaces were associated with a higher intraocular pressure. This means that gathering information about the corneal power of the posterior surface in a cataract surgery patient, may help to understand the

unique indices provided by ORA (CH and IOPcc). The change of biomechanical properties during cataract surgery is influenced significantly by preoperative biometric parameters such as corneal thickness and axial length. From a biomechanical point of view, cataract surgeons should not solely rely on tomographic examinations, but also consider corneal compensated IOP, especially in follow-up studies after cataract surgery.

2. INTRODUCTION

2.1 Optical system of the eye

Light refraction occurs at the boundary layers of structures with different optical properties. With respect to the eye, light refraction occurs at these five interfaces: 1) the air – tear film, 2) the tear film – anterior corneal surface, 3) the posterior corneal surface – aqueous humor, 4) aqueous humor – anterior lens surface and 5) the posterior lens surface – vitreous humor (**Figure 1**).

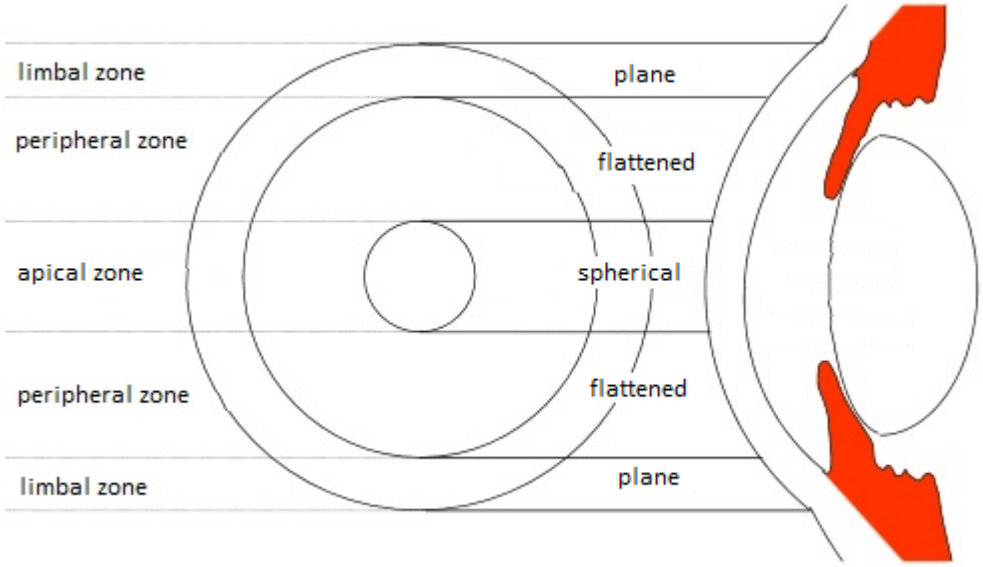

***Fig. 1**: The optical structure of the eye with the three different topographic zones of the cornea* [37].

The sum of all refractions provides the total optical power of the eye due to the different structures of the optical system of the eye. The total optical power in the relaxed adult eye is approximately 60 diopters (DPT). While the cornea accounts for about 2/3, or on average 40 DPT, the crystalline lens contributes the remaining one third (20 DPT) [22].

The cornea is of major importance for the image projected by the retina. It's form, the curvature of the anterior and posterior surfaces as well as the corneal thickness determines the refraction and course of a light beam entering the eye. The cornea provides an optical window for the eye and together with the adjacent sclera, which

has a smaller curvature, it is a part of the form and fibrous protective capsule of the eyeball. It's structure is robust and transparent and can be modulated. A precise retinal projection is only guaranteed by an optimally smooth corneal surface and adequate curvatures of the anterior and posterior surfaces.

2.2 Optics of the cornea

The Limbus corneae is the most peripheral zone of the cornea and functions as the interface with the sclera. This approximately 1 mm wide circular limbal zone is the origin of stem cells for the corneal epithelium and endothelium and is responsible for their continuous renewal. In a transverse direction the cornea has an oval shape. In adults the corneal diameter averages 11.5 mm vertically and 12 mm horizontally. The shape is meniscus like with a central thickness of 0.6 mm (0.4 – 0.8 mm) and a peripheral thickness of 1 mm (0.9 – 1.2 mm). The radius of the curvature is approximately 7.55 – 8.05 mm [1, 6, 45]. Astigmatism occurs if the vertical and horizontal radii differ significantly (corneal deformation of the curvature). The cornea can be divided into three zones, which are not clearly demarcated from one another (**Figure 1**). The apical zone in the center has a diameter of 4 – 5 mm and is the most important corneal zone for vision. The peripheral zone is the part of the cornea shadowed by the iris. The most peripheral limbal zone is not used for vision [37].

2.3 Anatomy of the cornea

The cornea is transparent and consists of the following layers (**Figure 2**):

. Epithelium

. Bowman's layer (Lamina limitans anterior)

. Stroma (Substantia propria)

. Descemet's membrane (Membrana limitans posterior)

. Endothelium

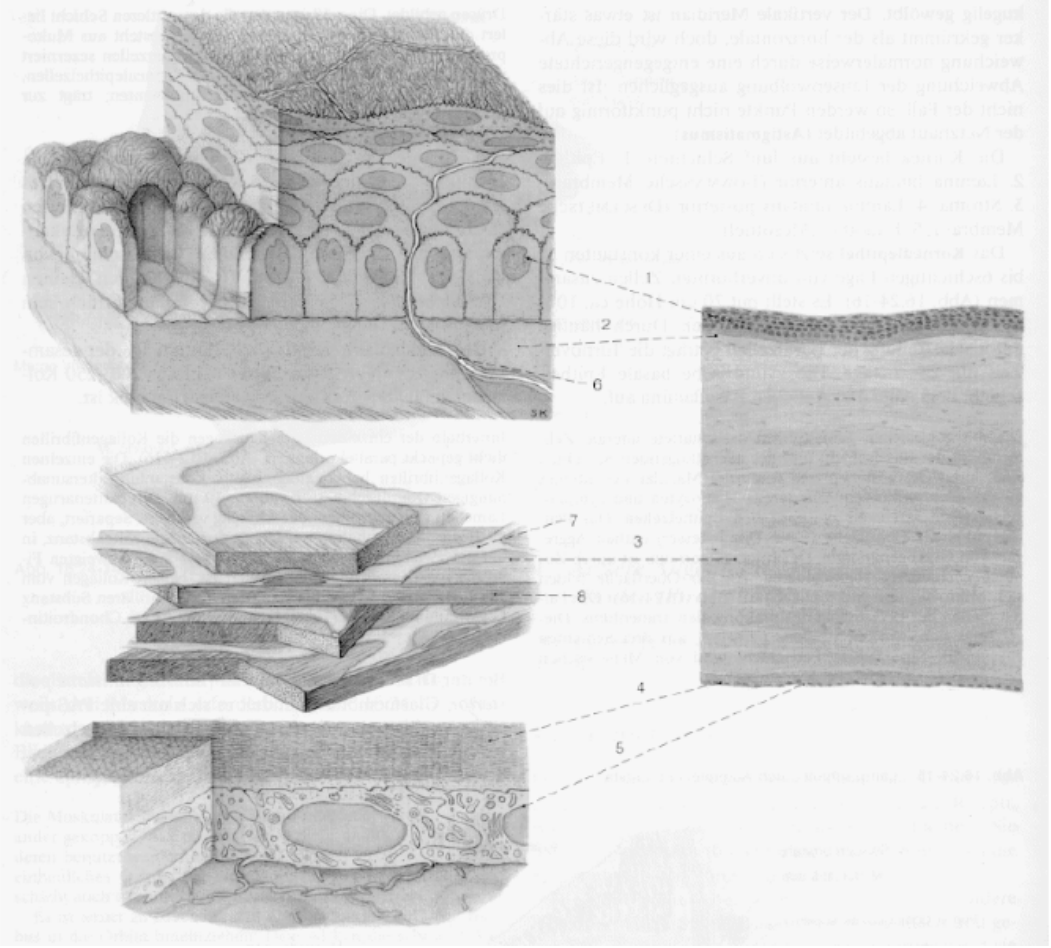

Fig. 2*: Corneal layers from the most anterior to the most posterior. 1) Epithelium, 2) Bowman's layer, 3) Stroma, 4) Descemet's membrane, 5) Endothelium, 6) Nerve, 7) Keratocytes, 8) Bundle of collagen fibrils* [2]*.*

2.3.1 Epithelium

The outermost layer of the cornea consists of non-keratinizing, multilayered squamous epithelial cells. The epithelium is 50 µm thick and represents ten percent of the corneal thickness [21]. The cells are arranged in 5 – 6 layers of three different cell types. At the corneal surface are 2 – 3 layers of flat epithelial cells. Below these are 2 – 3 layers of pterygocytes and a single layer of basal cells, which is bound to the basal membrane by hemidesmosomes. These layers make the corneal epithelium resistant to mechanical stress, for example eye rubbing. Only the basal cells can proliferate. It takes newly formed cells 7 – 14 days to migrate to the corneal surface. In this process the cells are transformed first into pterygocytes and then surface epithelium. After a cycle of a few days at the surface, the cells are

eventually shed off into the tear film. Continued regeneration of the corneal epithelium is provided by basal layers of the peripheral limbus and its stem cells [21]. The cells closest to the corneal surface are arranged in 2 – 3 layers of fully differentiated, squamous epithelial cells, which appear polygonal and flat (**Figure 3**).

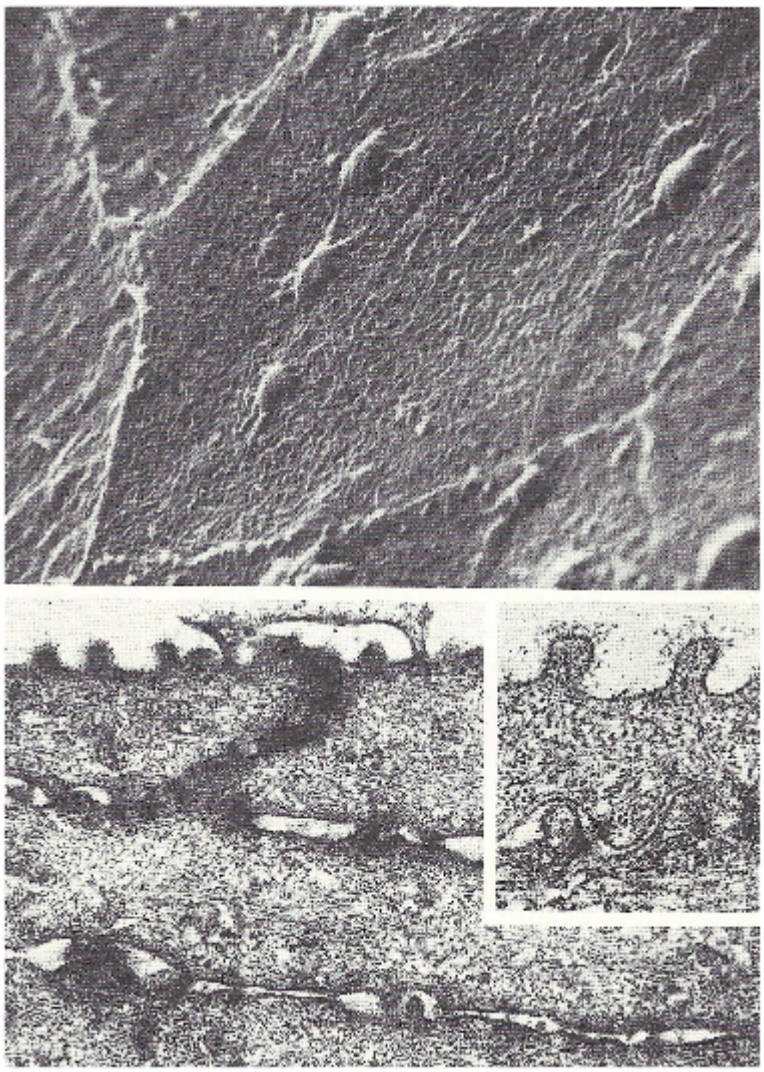

Fig. 3*: Detailed structure of corneal epithelial cells as seen by electron microscopy. Top: the superficial layer consists of flat polygonal cells [3]. Bottom: presentation of the 2 – 3 layer arrangement of epithelial cells with microfolds and microvilli, and the Glycokalix [4].*

The cells have a diameter of 40 – 60 µm and are 2 – 6 µm thick [25]. The surface of the outermost cells appears smooth. However, electron microscopy actually reveals a surface with microfolds and microvilli. This structural change increases the cell surface, thereby optimizing oxygen supply and exchange of nutrients between the cells and the tear film. The epithelial cell membrane consists of a double lipid layer that contains deposits of glycoproteins and glycolipids, which in turn are bound to glycosaccharides. This structure, the Glycokalix, facilitates the accumulation of mucin from the tear film through its hydrophobic properties. A closer look through the electron microscope reveals two very distinct cell types: dark, large opposed to lighter, smaller cells. The darker cells contain many microvilli. They are fully matured and are shed into the tear film. The lighter cells are younger and have fewer microfolds. Below, the fully differentiated surface epithelium consists of 2 – 3 layers of pterygocytes. They are less differentiated and have many desmosomes and gap junctions, which serve as cellular interconnections. Compared to basal cells they have fewer cellular components, but are rich in tonofilaments. The basal cells are attached to the basal membrane in a single layer. They possess a highly prismatic form with vertically arranged nuclei and represent 35 – 40% of the total epithelial thickness of the cornea. They are the only cells, which can divide. The cell system of the cornea is also of immunologic significance. Specialized macrophages (dendritic cells = Langerhans cells) are positioned near the limbus in the peripheral corneal epithelium and elicit an immune reaction in response to contact with a foreign antigen [6].

2.3.2 Bowman's layer (Membrana limitans anterior)

The Bowman's layer, also called Lamina limitans anterior, is an acellular layer beneath the corneal epithelium. In the adult it is approximately 8 – 12 µm thick and consists of collagen fibrils and proteoglycans primarily of type I, III, V and VII, whose filaments specifically support epithelial adhesion [56]. These collagen fibers have a diameter of approximately 25 nm and represent the most anterior portion of the corneal stroma [56]. They are combined in lamellae, which are arranged in a nonparallel spatial organization. The collagen fibrils of Bowman's layer have a smaller diameter than the fibrils of the stroma and contain numerous lamellar insertions, which ensure adhesion between Bowman's layer and the underlying

stroma [36]. An injury to this layer of the cornea will always result in scarring. The function of Bowman's layer is not entirely clear. However, it has been hypothesized that it serves to preserve corneal structural integrity and functions as a barrier against viral and tumor penetration.

2.3.3 Corneal stroma (Substantia propria)

This layer represents 95 per cent of the corneal volume and comprises an extracellular matrix, keratocytes (corneal fibroblasts) and nerve fibers. The cellular components represent only 2 – 3 per cent of the stroma. By far the largest component is the extracellular matrix, which consists mostly of collagen and glucosaminoglykanes, whereby collagen represents 70 per cent of the dry weight of the cornea [33]. The predominant stromal collagen is type I, but types III, V and VI are also present [25]. The collagen fibrils of a lamella have a diameter of approximately 0.2 – 2.5 µm and consist of a denser meshwork in the anterior third of the stroma. In contrast, the fibrils are thicker with a comparatively less dense meshwork in the posterior stroma [24]. The fibrils within each lamella are oriented in the same direction and run parallel to the corneal surface (**Figure 4**).

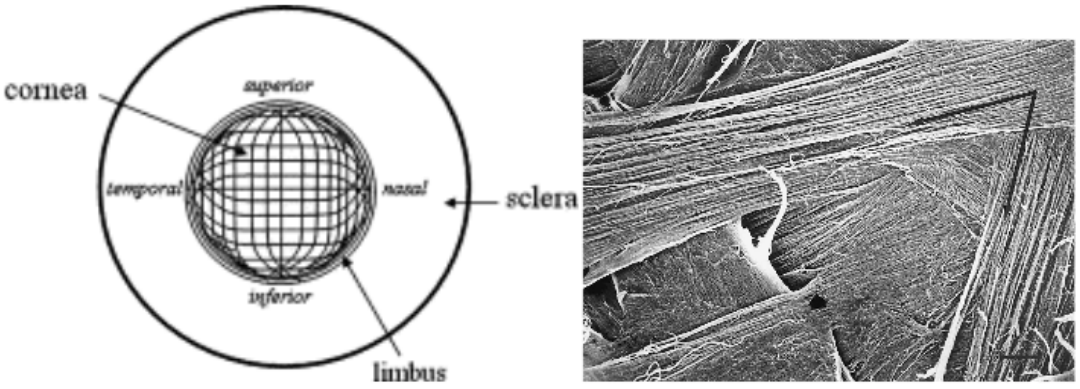

***Fig. 4**: On the left: The human cornea collagen fibrils show an orthogonal arrangement in the superior-inferior and the temporal – nasal planes [38]. On the right: Electron microscopic view of collagen fibrils in the middle stroma. The arrow (upper right) indicates the crossing angle of two lamellae [10].*

With an angle of 90 degrees in both planes, the temporal-nasal and superior-inferior, the orientation of the lamellae varies between adjacent layers [8]. This arrangement is particularly visible in the posterior two thirds of the stroma [1]. The collagen fibrils form a peripheral ring at the limbus (**Figure 4**). By being incorporated into the sclera, the fibers contribute to the structural integrity of the limbal area [35]. The collagen fibrils in the human stroma have a uniform diameter of 22.5 – 35 nm. The distance between fibrils is also constant at 41.4 ± 0.5 nm [25].

With increasing age, collagen molecules increase in size and intermolecular spaces widen (cross linking) [12] leading to three-dimensional growth of collagen fibrils. The collagen fibrils form approximately 300 lamellar layers within the stroma [25]. This arrangement is particularly important for the biomechanical properties of the cornea. The collagen fibrils are surrounded by glucosaminoglykanes, which consist primarily of keratansulfate (65%), chondroitinsulfate and dermatansulfate [25]. Glucosaminoglykanes form chains of disaccharides, which in turn form proteoglycans by binding with a covalent bond to a relatively plain protein, the core-protein. A number of different models have been proposed to explain the proteoglycan–collagen interaction. The most recent studies suggest a non-rigid bond between collagen fibrils and proteoglycans, which would promote optimal supply of oxygen and nutrients as well as cell migration [23]. In the case of wound healing or other regenerative processes in the cornea, the keratocytes located between the stromal lamellae can be transformed into fibroblasts, capable of synthesizing glucosaminoglykanes and a preliminary stage of collagen fibrils. Keratocytes also produce enzymes, such as metalloproteases, which aid in breaking down collagen. These processes of cell regulation preserve the structural and biochemical homoeostasis of the extracellular matrix [25]. The corneal stroma lacks blood or lymphatic vessels, although a few nerve fibers, branches of the Nervi ciliares, can be found in the most anterior portion of the stroma.

2.3.4 Descemet's membrane (Membrana limitans posterior)

Descemet's membrane is the thickest membrane of the human body. Throughout the course of life, its thickness increases from 3 µm at birth to 8-10 µm in an adult. It is believed to be derived from the endothelial cells. Three different histological

components can be identified: an outer layer adjacent to the Substantia propria (0.3 µm), an anterior layer (2 – 4 µm), and an inner layer adjacent to the endothelium. The latter has virtually no fibrillary components and is approximately 5 µm thick. This layer is also the reason for the increase in thickness of Descemet's membrane from infancy to adulthood [25]. Following injury, the Descemet's membrane is regenerated by the endothelium. Immuno-histochemical studies have revealed the presence of fibronectin, type IV collagen and laminin [7].

2.3.5 Endothelial cell layer

The corneal endothelium consists of a single layer of flat hexagonal cells, which are held together by the "Zonulae adhaerentes". The cells are 5 µm thick and 20 µm wide [5]. The gap junctions between the cells are oriented towards the anterior chamber and are filled with protein complexes, except for a narrow space of 3 – 4 nm, which allows water and ions to pass through the gap. The endothelium is therefore not a watertight cell structure but functions as a bidirectional transport system for water and ions. The pumping mechanism is primarily related to Na+/K+ - ATPase action. The main function of the endothelium is the maintenance of the corneal transparency as well as the hydration of the substantia propria (78%) and the epithelium through hydrostatic pressure of the inner eye and the anterior chamber. Interruptions of the pump function lead to fluid accumulation in the layers of the cornea (corneal edema) and, thus, to decreased transparency. In a healthy individual the endothelial pump mechanism can overcome a hydrostatic pressure of up to 40 mm Hg [28].

2.4 Cataract

A cataract (German language synonym: Grauer Star) refers to an opacity issue of the lens, which results in decreased transparency, often beginning with radial vacuoles, which causes the patient to notice foggy vision. Diminished visual acuity can be verified objectively by the usual examinations. The degree of reduced vision depends on the extent and position of the lens opacity. The term cataract was originally derived from the Greek word Katarractes, which means waterfall. In the German language the Latin, feminine form (die Katarakt) is used. The German term, Grauer Star, is based on the fixed stare of patients with cataracts who have become blind [15].

Prior to modern medical insights into this disorder, it was widely believed that a cataract was the result of coagulated fluid from the brain, which would then accumulate behind the pupil.

2.4.1 Epidemiology

A cataract is the most common disease of the lens [15]. Similarly, cataract surgery is the most successful and most frequently performed eye surgery. In Germany alone 800,000 cataract surgeries were performed in 2007 [56]. On a global level, cataracts are the most common cause of blindness [57].

2.4.2 Cataract classification

Cataracts are usually separated into four categories and classified as congenital, juvenile, pre-senile or senile, each depending on the age of onset, extent and etiology. Pre-senile cataracts begin between adolescence and middle age. They are progressive and eventually lead to diminished visual acuity. They have also been described as early onset senile cataracts. Senile cataracts (grauer Altersstar) represents a physiologic aging process with generally slow progression and a persistently clear lens cortex, which makes it difficult to differentiate from other normal changes resulting from advanced age, which may lead to a nuclear sclerosis of the lens.

2.5 Cataract Surgery (Phacoemulsification) and implantation of a posterior chamber lens

Cataracts as a disease have been known since the antiquity. Archeological findings suggest that methods were developed thousands of years ago to move the cataract away from the optical axis with needles. The first known cataract surgery (couching technique) was presumably done in Egypt [32] (**Figure 5**).

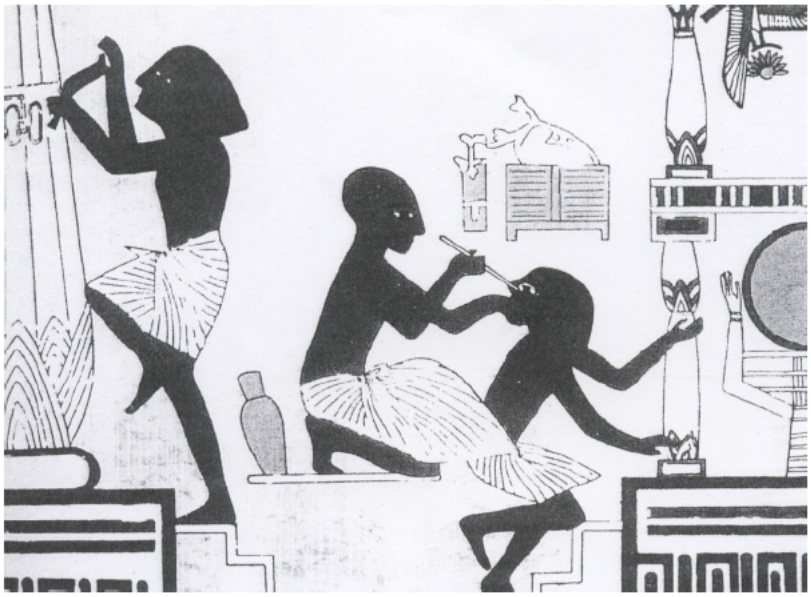

Fig. 5*: Egyptian wall painting, approximately 1200 BC. An Oculist treats the eye of a worker. It is uncertain whether this picture is the first presentation of a cataract operation or not* [32]*.*

2.5.1 Surgical technique

Nowadays cataract surgery is primarily carried out as an outpatient procedure (US 99%, EU 84%) [42]. The pupil is dilated prior to surgery. In order to ensure postoperative wound stability and intraoperative safety, self-sealing “tunnel incisions”, which do not require sutures, are made either in the sclera or cornea. The classical access to cataract extraction is superior. However, more frequently a lateral position of the incision has been employed (US 65%, EU 32%) [42]. In the presence of a corneal astigmatism, altering the course and localization of the incision on the steep corneal meridian will lead to a decrease in the curvature of the cornea [57]. These new access techniques result in incisions of less than 2.8 mm. The standard method for cataract extraction is currently phacoemulsification. A hollow needle (phaco hand-piece), which vibrates at a high frequency (ultrasound), is inserted into an opening created in the anterior lens capsule. The ultrasound breaks down the lens material, which can then be removed by aspiration (**Figure 6**).

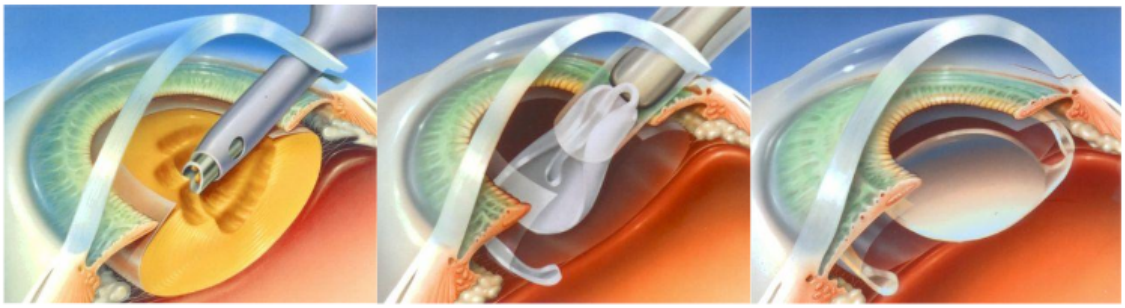

***Fig. 6**: Cataract surgery (http://ocunet.de/patienten/grauer_star.html)*

During the operation, the corneal endothelium is protected by intraocular injection of dispersive or cohesive viscoelastic material that also improves the operative field for the surgeon [32].

2.5.2 Intraocular lenses (IOLs)

Modern standard IOLs are predominantly spherical lenses, which correct the spherical equivalent of the aberrations of the aphakic eye (total refractive IOL power 10 – 30 DPT). The power and size of the aspherical IOL depends on its localization (capsule or sulcus ciliares) and the desired lens function (postoperative refraction target). The typical IOL-optic is 6 mm long with a total haptics length of 12 – 13 mm. The different IOL types are: rigid polymethyl-methacrylate IOLs, foldable silicon IOLs and hydrophobic or hydrophilic acrylic IOLs. Foldable IOLs are more popular now because they do not require incisions more than 3mm. In 2007 less than 1% rigid IOLs were used in Germany and incision width was less than 2.8 mm [56]. Nowadays, IOLs are produced with sharp back edges to decrease posterior capsule opacity after cataract surgery (so-called “Nachstar”). This design prevents the cells from migrating into the central posterior capsule and thus a recurrence of opacity in the optical axis. Aspherical IOLs have an optimized surface curvature, which makes them perfectly suitable for correcting the spherical high order aberrations. These IOLs lead to an improved visual acuity and contrast sensitivity particularly in patients with large pupils [25].

Since short wave spectrum is suspected to induce macular degeneration through photo oxidative damage, blue filter (yellow) intraocular lenses are used to reduce the transmission of the shortwave spectrum of light. Moreover, it is known that the effect

of chromatic aberration leads to a greater dispersion of short wave light in comparison to longer wavelength light, which often leads to diminished contrast sensitivity. It is astonishing that in 2007 approximately 72% of the German surgey centers implanted only 100 blue filter IOLs, in contrast to 8% of centers in other countries that implant more than 500 per year [56].

2.5.3 Results of cataract surgery

The success of a cataract surgery is primarily measured by the long-term improvement of visual acuity and also by the lack of complications during surgery. Visual acuity is tested primarily by examination of the high contrast sharpness of vision (visual acuity) and the residual refraction deficit of the implanted lens [43]. While visual acuity can be evaluated easily and quickly, it does not provide a complete examination of the complexity of visual perception. Therefore “optical quality” has been introduced, which evaluates the ability to see well under different light conditions. Optical quality is determined by combining the results of a number of subjective and objective tests [43].

2.6 Ocular Response Analyzer (ORA)

The ocular response analyzer measures the biomechanical properties of the cornea. It functions in a similar manner as the pneumo-tonometer and evaluates the elastic properties of the cornea. Elastic materials react proportional to an applied force, which makes their deformation independent of the speed or time course of the applied force. Viscous materials, on the other hand, have a deformation that is dependent on speed and time course of the force applied. Since the cornea is a viscoelastic tissue, it combines both properties [11.] The ORA is suitable for testing the dual nature of the cornea because it combines a device for imparting a rapid air impulse onto the cornea with a pressure transducer and an advanced electro-optical system (**Figure 7**).

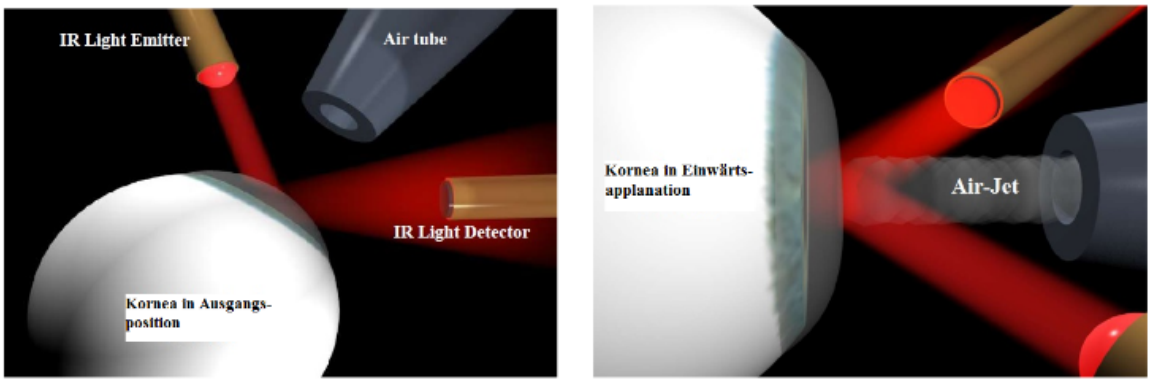

***Fig 7**: Operating principle of the Ocular Response Analyzer [21].*

The pressure of the air impulse causes the cornea to react in a concave deformity, which then returns to its original state. During this indentation and relaxation process the cornea is in a plane position for short periods, a process that has been called bidirectional applanation [18]. By measuring the reflection of infrared light, the time course and degree of corneal deformation are determined. This information about the strength of the air impulse and the corneal deformation is automatically analyzed and printed out as a bio-corneogram (**Figure 8**) [26].

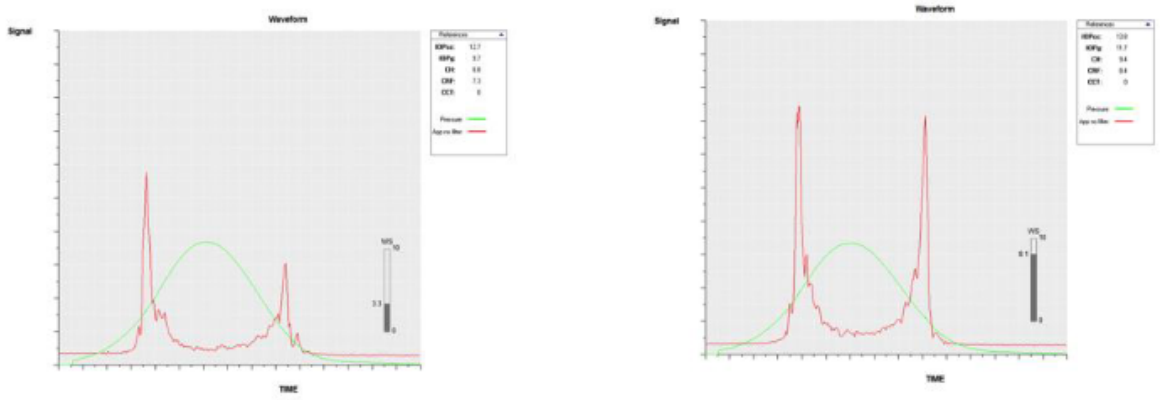

***Fig. 8**: Biocorneograms. The green curves represent the pressure generated by the rapid air pulse to deform the cornea. The red curves represent the raw signal of the applanation detection system. The peaks of these curves indicate the reflection of the infrared light during the in- and out applanation [22].*

Both applanation pressures, P1 and P2, are represented by the pressures at the two peaks of the applanation curves, during in and out applanation. The viscoelastic

properties of the cornea dictate that lower pressure is required for outward movement than for inward movement [26.] The difference between the two applanation pressures is called corneal hysteresis (CH). Hysteresis refers to the delay in the response time of a material to a change in force application. The hysteresis of the cornea depends on its viscous damping properties, which are the direct result of the viscosity of the cornea and effects of the collagen matrix. CH describes the delay between the in- and out movement of the cornea in response to pressure. Another parameter derived from the ORA is the corneal stiffness or corneal resistance factor (CRF). It measures the total resistance of the cornea to deformation and depends on the damping properties and the elastic resistance to force application. The means of two separate applanation measurements is an index of intraocular pressure, IOPg. This result can be compared with the results of another instrument, the Goldmann tonometer, the gold standard method of intraocular pressure measurement. Another derived parameter is the IOPcc (the corneal independent intraocular pressure), which provides results that are not as heavily influenced by corneal properties as other comparable measurements [39, 40].

2.7 Hypothesis and purpose of the study

The objective of this study is to investigate the changes of the corneal biomechanical properties in terms of CH, CRF, IOPg and IOPcc measurements made with the Ocular Response Analyzer and to analyze potential influencing factors from biometry, corneal topography and endothelial cell measurements.

3. PATIENTS AND METHODS

3.1 Study group and protocol [48, 49]

This prospective consecutive cross sectional study involved 54 eyes with cataract in stages I or II with visually significant lens opacity that were treated with phacoemulsification (2.8 mm incision) from May 2012 to January 2013.

Inclusion criteria were: Patients between 40 and 80 years old with at least one cataract eye, no history of previous ocular surgery nor pathologies, and the presence of a normal fundus. Exclusion criteria were astigmatism exceeding more than 3.00 diopters (DPT) or the need of any other ocular surgery.

The study followed the tenets of the Declaration of Helsinki, and the local ethics committee of our university approved the study protocol. The procedures, risks, and potential complications of the study were thoroughly explained with each patient, and all patients signed written informed consent forms.

3.2 Surgical technique [48, 49]

All phacoemulsification cataract surgeries were performed by the same surgeon (M.E.H.) using retrobulbar anesthesia. A clear corneal incision (CCI) with a width of 2.8 mm was created using a corneal keratome at the steep meridian either temporally or superiorly. At 90 degrees from the main incision, two paracenteses, smaller than 0.9 mm, were performed with the corneal keratome. The capsulorhexis was performed using a capsulorhexis forceps after Healon Ophthalmic Viscosurgical Device (OVD, Abbott Medical Optics, Illinois, USA) was injected into the anterior chamber. Hydrodissection and hydrodelineation were performed using balanced saline solution. By the means of the stop-and-chop technique, phacoemulsification (Alcon Infiniti®, Alcon, Texas, USA) was carried out. The residual cortex was removed by the bimanual irrigation and aspiration instruments. Thereafter, Healon was once again injected in the anterior chamber to enable the foldable intraocular lens (IOL) implantation. After that, Healon was aspirated bimanually. Hydration of the CCI and the two paracenteses was performed to tightly seal the wounds. Postoperative topical ofloxacin 0.3% and prednisolone acetate 1% were used routinely.

3.3 Patient examination [48, 49]

All patients were subjected to full ophthalmic examinations including slit-lamp examination, examination of the posterior segment of the eye, and visual acuity evaluation using Snellen charts, topography and tomography with Topographic Modeling System TMS-5 (TOMEY corp.) and CASIA (TOMEY corp.), biometry testing with the IOL Master (Carl Zeiss Meditec), corneal endothelium imaging performed with a specular microscope EM-3000 (TOMEY corp.), and examination of biomechanical properties performed with the ORA (Reichert, Inc., software version 3).

Together with all other ophthalmic examinations, ORA testing was carried out between 7 a.m. and 10 a.m., to avoid diurnal fluctuation stated by the manufacturer.

Standardized postoperative examinations were performed before the cataract surgery and 4 weeks post-surgery to minimize the effect of wound healing on the biomechanics.

3.4 Main outcome measures [48, 49]

The following biometric characteristics were derived from corneal topography: anterior equivalent (EQ_{TMS}) and cylinder (CYL_{TMS}) power. Biometric characteristics derived from corneal tomography included: anterior and posterior equivalent (EQ_{aCASIC}, EQ_{pCASIA}) and cylinder (anterior and posterior cylinder (CYL_{aCASIA}, CYL_{pCASIA}) power. Biometric characteristics derived from keratometry included: anterior equivalent (EQ_{IOL}) and cylinder (CYL_{IOL}) power. Biometric characteristics derived from the autorefractor included: anterior equivalent (EQ_{AR}) and cylinder (CYL_{AR}) power. Corneal hysteresis (CH), corneal resistance factor (CRF), Goldmann-related intraocular pressure (IOPg), and corneal compensated intraocular pressure (IOPcc) were assessed with the ORA preoperatively and again 1 month after the surgery. Results from ORA were analyzed and correlated with those from all other examinations that were carried out at the same time in a cross-sectional manner. In addition, all measurements from the TMS-5, biometric characteristics of IOLMaster and endothelial cell measurement were recorded. As outcome measures, we restricted those parameters, which showed a statistically significant effect on

biomechanical properties change. TMS-5: CSI and SAI preoperative; IOLMaster: AL preoperative; EM-3000: CCT and ECC preoperative.

3.5 Statistical analysis [48, 49]

Statistical analysis was performed using the SPSS statistical software package for Windows (version 19.0, SPSS, Inc.). Data was expressed descriptively by mean ± standard deviation (SD), median and range. In a correlation analysis, Pearson rank correlation coefficient r was used to identify the significant biometric parameters, which could potentially affect the biomechanical properties before and after cataract surgery. In addition, the impact of biometric parameters on the changes of biomechanical outcome measures was assessed using Pearson rank correlation coefficients. A p-value less than 0.05 was considered mild statistically significant, less than 0.01 moderate statistically significant and less than 0.001 strong statistically significant, without taking the r-value into consideration.

4. RESULTS

Biomechanical properties and biometric characteristics (preoperative and postoperative) are further described in **Table 1**.

The impact of biometric characteristics on biomechanical properties (**preoperative**) is shown in **Table 2.** At the preoperative examination stage, corneal hysteresis CH showed a moderate negative correlation with EQ_{pCASIA}, a moderate positive correlation with CYL_{pCASIA} and a mild positive correlation with CYL_{TMS}, EQ_{aCASIA} and CYL_{aCASIA}. This leads to the conclusion, that a flatter corneal back surface is linked with a higher corneal hysteresis. All other preoperatively measured biometric characteristics, which were not significantly correlated with biomechanical properties, are also presented in **Table 2**.

The impact of biometric characteristics on biomechanical properties (**postoperative**) is shown in **Table 3.** At the postoperative examination stage, CH showed a mild positive correlation with EQ_{aCASIA} and EQ_{AR} and a mild negative correlation with EQ_{pCASIA} and EQ_{TMS}. This leads to the conclusion that a steeper corneal front surface and a flatter corneal back surface are linked to a higher corneal hysteresis. Both IOPcc and IOPg showed a strong to moderate negative correlation with EQ_{TMS}, respectively, moderate to mild negative correlation with EQ_{IOL}, respectively, mild negative correlation with EQ_{AR}, moderate negative correlation with EQ_{aCASIA} and a strong to moderate positive correlation with EQ_{pCASIA}, respectively. That means, that steeper corneal front and back surfaces are associated with a higher intraocular pressure. All other postoperatively measured biometric characteristics, which were not significantly correlated with biomechanical properties, are also presented in **Table 3**.

Intercorrelation among corneal power values (preoperative and postoperative) from different devices is shown in **Table 4.** EQ_{TMS}, EQ_{IOL}, EQ_{AR}, EQ_{aCASIA} and EQ_{pCASIA} were significantly correlated with each other both before and after surgery.

Intercorrelation among corneal astigmatism (preoperative and postoperative) from different instruments is shown in **Table 5**. CYL_{TMS}, CYL_{aCASIA}, CYL_{pCASIA}, CYL_{IOL}, and CYL_{AR} were significantly correlated with each other both before and after surgery [49].

Table 6 describes the biomechanical changes from the examination results before and one month after surgery. Mean changes in the biomechanical measurements were ΔCH = -0.45 mmHg, ΔCRF = -0.88 mmHg, ΔIOPg = -1.58 mmHg and ΔIOPcc = -0.35 mmHg.

Potential predictive biometric parameters for the change of biomechanical values (1 month postoperatively versus preoperatively) are shown in **Table 7.** The predictive values are based on a model using multiple linear regression, which is restricted to just the relevant dependencies. ΔCH, the average value of which was negative, showed a linear dependency on CSI, indicating that a large CSI value is affecting a smaller decrease of CH due to cataract surgery. Average value of ΔCRF was negative, which showed a linear dependency on CCT, indicating that a large CCT value refers to a larger decrease of CRF due to surgery. Mean value of ΔIOPg was negative, and ΔIOPg showed a linear dependency on AL, indicating that a large AL value refers to a smaller decrease of IOPg due to surgery. ΔIOPcc, the average value of which was negative, showed a linear dependency on AL, SAI and ECC, indicating that large AL, SAI and ECC value are affecting a smaller decrease of IOPcc due to cataract surgery [48].

Table 1. ***Descriptive information for biomechanical properties and biometric characteristics pre- and 1 month postoperative*** [49]

		Preoperative			1 month Postoperative		
		Mean ± SD	Median	Range	Mean ± SD	Median	Range
Biomechanical values	CH [mmHg]	10.38 ± 1.38	10.60	6.90 - 13.00	9.91 ± 1.30	9.80	6.30 - 13.10
	CRF [mmHg]	10.57 ± 1.35	10.55	7.10 - 13.60	9.71 ± 1.03	9.70	7.70 - 12.00
	IOPcc [mmHg]	16.05 ± 4.61	15.90	2.80 - 27.20	15.81 ± 3.98	16.00	8.60 - 23.90
	IOPg [mmHg]	16.11 ± 4	15.90	7.50 - 25.30	14.64 ± 3.56	14.50	8.20 - 22.10
Biometric chracteristics	EQ_{TMS} [D]	43.88 ± 2.25	43.73	41.22 - 46.33	43.68 ± 1.23	43.70	41.16 - 47.08
	CYL_{TMS}[D]	0.22 ± 0.22	0.15	0 - 1.20	0.17 ± 0.13	0.13	0 - 0.54
	EQ_{IOL} [D]	43.34 ± 1.4	43.12	40.84 - 47.43	43.31 ± 1.40	43.05	40.84 - 47.43
	CYL_{IOL} [D]	1.07 ± 0.95	0.78	0 - 2.18	1.04 ± 0.94	0.76	0 - 2.06
	EQ_{AR} [D]	44.05 ± 1.29	43.88	41.38 - 46.75	44.39 ± 2.05	44.00	41.75 - 46.25
	CYL_{AR} [D]	1.01 ± 0.89	0.75	0 - 3.75	1.06 ± 0.99	0.75	0 - 5.50
	EQ_{aCASIA} [D]	43.66 ± 16.47	43.98	41.5 - 47.35	44.06 ± 1.27	44.00	41.75 - 46.50
	CYL_{aCASIA} [D]	0.98 ± 0.86	0.70	0.10 - 3.80	1.01 ± 0.73	0.80	0.20 - 3.10
	EQ_{pCASIA} [D]	-6.18 ± 0.23	-6.18	-6.35 - -6.05	-6.20 ± 0.23	-6.20	-6.22 - -6.17
	CYL_{pCASIA} [D]	0.33 ± 0.21	0.30	0.10 - 1.30	0.33 ± 0.20	0.30	0.10 - 0.80

Table 2. *Impact of biometric characteristics on the preoperatively measured biomechanical properties*

		CH	CRF	IOPcc	IOPg
EQ_{TMS} [D]	r value	0.033	0.088	0.103	0.065
	p value	0.814	0.529	0.461	0.641
CYL_{TMS}[D]	r value	**0.293***	0.209	-0.099	-0.051
	p value	0.031	0.129	0.477	0.716
EQ_{IOL} [D]	r value	0.215	0.052	-0.149	-0.155
	p value	0.118	0.709	0.282	0.263
CYL_{IOL} [D]	r value	0.203	0.007	-0.243	-0.187
	p value	0.140	0.962	0.077	0.177
EQ_{AR} [D]	r value	0.231	0.080	-0.140	-0.139
	p value	0.092	0.567	0.312	0.317
CYL_{AR} [D]	r value	0.201	0.114	-0.132	-0.064
	p value	0.145	0.413	0.340	0.645
EQ_{aCASIA} [D]	r value	**0.201***	0.114	-0.132	-0.064
	p value	0.033	0.368	0.422	0.237
CYL_{aCASIA} [D]	r value	**0.28***	-0.128	-0.106	-0.157
	p value	0.04	0.358	0.444	0.255
EQ_{pCASIA} [D]	r value	**-0.434****	-0.213	0.181	0.189
	p value	0.001	0.122	0.190	0.172
CYL_{pCASIA} [D]	r value	**0.419****	0.248	-0.229	-0.128
	p value	0.002	0.071	0.096	0.357

Significant values are shown in bold.
*/ ** refers to mild/ moderate or strong statistically significant correlation.

Table 3. *Impact of biometric characteristics on the 1 month postoperatively measured biomechanical properties*

		CH	CRF	IOPcc	IOPg
EQ_{TMS} [D]	r value	**-0.281***	0.180	**-0.457****	**-0.447****
	p value	0.038	0.188	<0.001	0.001
CYL_{TMS}[D]	r value	0.116	0.052	-0.086	-0.055
	p value	0.397	0.708	0.532	0.687
EQ_{IOL} [D]	r value	0.248	-0.090	**-0.348****	**-0.326***
	p value	0.068	0.514	0.009	0.015
CYL_{IOL} [D]	r value	0.179	0.120	-0.099	-0.043
	p value	0.190	0.381	0.472	0.753
EQ_{AR} [D]	r value	**0.273***	-0.035	**-0.329***	**-0.311***
	p value	0.043	0.801	0.014	0.030
CYL_{AR} [D]	r value	0.043	0.010	-0.042	-0.031
	p value	0.756	0.944	0.760	0.824
EQ_{aCASIA} [D]	r value	**0.043***	0.010	**-0.042****	**-0.031****
	p value	0.021	0.624	0.003	0.007
CYL_{aCASIA} [D]	r value	0.055	0.058	-0.013	0.009
	p value	0.690	0.673	0.926	0.948
EQ_{pCASIA} [D]	r value	**-0.307***	0.154	**0.454****	**0.436****
	p value	0.022	0.262	<0.001	0.001
CYL_{pCASIA} [D]	r value	0.129	-0.100	-0.215	-0.213
	p value	0.348	0.468	0.114	0.119

Significant values are shown in bold.
*/ ** refers to mild/ moderate or strong statistically significant correlation.

Table 4. *Intercorrelation among corneal power values (preoperative and postoperative) from different devices* [49]

		EQ_{TMS}	EQ_{IOL}	EQ_{AR}	EQ_{aCASIA}	EQ_{pCASIA}
EQ_{TMS}	r value		**-0.862****	**-0.420****	**-0.944****	**0.525****
	p value		<0.001	0.002	<0.001	<0.001
EQ_{IOL}	r value	**-0.652****		**0.398****	**0.925****	**-0.654****
	p value	<0.001		0.003	<0.001	0.002
EQ_{AR}	r value	**-0.696****	**0.934****		**0.454****	**-0.779****
	p value	<0.001	<0.001		0.001	<0.001
EQ_{aCASIA}	r value	**-0.709****	**0.914****	**0.974****		**-0.804****
	p value	<0.001	<0.001	<0.001		0.001
EQ_{pCASIA}	r value	**0.542****	**-0.808****	**-0.853****	**-0.882****	
	p value	<0.001	<0.001	<0.001	<0.001	

Data shown in the lower left part of the table are the before surgery calculated results, while data in the upper right part reflect the results from 1 month after surgery.

Significant values are shown in bold.

** refers to moderate or strong statistically significant correlation.

Table 5. *Intercorrelation among corneal astigmatism values (before and after surgery) from different devices* [49]

		CYL_{TMS}	CYL_{IOL}	CYL_{AR}	CYL_{aCASIA}	CYL_{pCASIA}
CYL_{TMS}	r value		**0.636****	**0.598****	**0.809****	**0.506****
	p value		<0.001	<0.001	<0.001	<0.001
CYL_{IOL}	r value	**0.609****		**0.763****	**0.614****	**0.873****
	p value	<0.001		<0.001	<0.001	<0.001
CYL_{AR}	r value	**0.716****	**0.899****		**0.895****	**0.772****
	p value	<0.001	<0.001		<0.001	<0.001
CYL_{aCASIA}	r value	**0.755****	**0.869****	**0.942****		**0.704****
	p value	<0.001	<0.001	<0.001		<0.001
CYL_{pCASIA}	r value	**0.800****	**0.676****	**0.725****	**0.768****	
	p value	<0.001	<0.001	<0.001	<0.001	

Data shown in the lower left part of the table are the before surgery calculated results, while data in the upper right part were recorded 1 month after surgery.

Significant values are shown in bold. ** refers to moderate or strong statistically significant correlation.

Table 6. *Changes of biomechanical properties from preoperatively to 1 month postoperatively* [48]

	ΔCH [mmHg]	ΔCRF [mmHg]	ΔIOPg [mmHg]	ΔIOPcc [mmHg]
Mean ± SD	-0.45 ± 1.27	-0.88 ± 1.1	-1.58 ± 3.15	-1.45 ± 3.93
Median	-0.5	-0.8	-1.4	-0.75
Min - max	-3.4 - 2.7	-3.1 - 1.7	-8.1 - 4.7	-13.1 - 6.6

CH = corneal hysteresis

CRF = corneal resistance factor

IOPg = Goldmann-correlated intraocular pressure

IOPcc = corneal compensated intraocular pressure

Table 7. *Potential predictive biometric characteristics for the changes of biomechanical parameters (1 month postoperative versus preoperative)* [48]

Change of biomechanical parameters / Biometric characteristics		Constant for regression formula	CSI	SAI	AL	CCT	ECC
ΔCH	Regression coefficient	-0.695	1.28	-	-	-	-
	r value	-	0.302	-	-	-	-
	p value	0.001	0.028	-	-	-	-
ΔCRF	Regression coefficient	6.072	-	-	-	-0.013	-
	r value	-	-	-	-	-0.371	-
	p value	0.03	-	-	-	0.013	-
ΔIOPg	Regression coefficient	-21.134	-	-	0.854	-	-
	r value	-	-	-	0.417	-	-
	p value	0.004	-	-	0.005	-	-
ΔIOPcc	Regression coefficient	-25.373	-	4.025	0.734	-	0.003
	r value	-	-	0.478	0.351	-	0.339
	p value	0.003	-	<0.001	0.01	-	0.013

A "-" marks parameters, which did not affect biomachanical properties.

Regression coefficient in first row of each ORA parameter is representative with a linear regression function. (e.g. ΔCH = -0.695 + 1.28 • CSI)

R value refers to correlation coefficient.

P values refers to significance level.

5. DISCUSSION

In this study, we evaluated biomechanical properties before and after phacoemulsification cataract surgery and correlated these findings with biometric characteristics such as equivalent and cylinder power of the cornea obtained from corneal topography, tomography and keratometry. Corneal thickness, curvature, and volume are the principal structural attributes of the cornea.

In addition, corneal properties can be characterized more comprehensively using biomechanical parameters such as CH and CRF. Two major causes for changes in the corneal biomechanical profile include pathologies like keratoconus and treatment-related corneal alterations [57]. The ocular response analyzer (ORA; Reichert Ophthalmic Instruments, Buffalo, NY) is the most common device used to evaluate the corneal biomechanical characteristics. The ORA combines rapid air impulse with an advanced electro-optic system to evaluate changes in the corneal shape by measuring the response to indentation. The corneal hysteresis (CH) and the corneal resistance factor (CRF) are the main biomechanical parameters derived through this deformation process. CH is a measure of corneal tissue properties that result from viscous damping, and CRF indicates the overall resistance of the cornea [56].

Corneal hysteresis is related to the viscoelastic structure of corneal tissue, which provides the cornea with its characteristic dampening effect [4]. Corneal curvature has also been shown to influence biomechanical features. A study by Lim et al showed a strong negative correlation between the CH value and maximum keratometry values in normal eyes. In that study the CH was lowered by 1 mm Hg per 6 diopters of corneal steepening [29].

The center surround index (CSI) is calculated from the difference in the average-area-corrected power between the central area (3.0 mm diameter) and an annulus surrounding the central area of the cornea. Together with the opposite sector index (OSI) and differential sector index (DSI), CSI aids in the differentiation between regular astigmatism (low value), normal corneas (low value), peripheral steepening keratoconus (low-middle value), and central steepening keratoconus (high value) [31]. Our study showed a positive correlation between the change of CH and CSI

(regression formula: $\Delta CH = -0.695 + 1.28 \cdot CSI$). The mean value of ΔCH was negative, which indicates that a cornea with a higher power difference between center and surrounding may potentially indicate a smaller decline in viscous damping capacity of the corneal tissue due to cataract surgery, which is predominantly determined by the concentration and viscosity of the glucosaminoglycans and proteoglycans in corneal stroma, as well as by the collagen-matrix interactions [57].

In addition to significant misalignment of the stromal collagen lamellae in keratoconus, microscopic and immunohistochemical studies have shown abnormal distribution of collagen types and alterations of the proteoglycans in stromal extracellular matrix [3, 34], which could partly explain these findings. Our data shows that even in normal corneas the change of CH due to cataract surgery depends significantly on the preoperative value of the CSI index. However, further research is required to focus on microscopic morphological changes under those conditions [48].

Focusing on the change of IOPg due to cataract surgery, we found a correlation with AL (regression formula: $\Delta IOPg = -21.134 + 0.854 \cdot AL$). Interestingly, the cornea independent IOPcc was correlated with AL, SAI, and ECC (regression formula: $\Delta IOPcc = -25.373 + 0.734 \cdot AL + 4.025 \cdot SAI + 0.003 \cdot ECC$). Both average values of ΔIOPg and ΔIOPcc were negative. For both regressions (IOPg and IOPcc), axial length was positively correlated with IOPg and IOPcc, indicating that an eye with larger axial length may be potentially associated with a smaller decline in IOP due to cataract surgery. In accordance with our research, Kucumen et al. found that the mean IOPcc was statistically significantly lower at 3 months than preoperatively [27]. In contrast, according to research of Alió et al., myopic eyes with higher extensibility and less resistance to the expansive force of normal IOP were accompanied with an increase in AL [4]. But the results of both studies are not comparable, because Alió et al. used a different population (myopic patient) compared to the present study (cataract patient), which excludes patients with other ocular disorders. Findings made by Cho showed, especially in myopic eyes (with a large AL), that the change in IOP due to cataract surgery was significantly increased [9].

Therefore, eyes with a large axial length may require more detailed monitoring of biomechanical properties and IOP postoperatively [9]. In general, a larger axial length

is associated with a flatter geometry of the IOL, typically a more posterior position within the eye, and a lower refractive power.

We also investigated the factors influencing the change of CRF, which reflects the elastic properties and rigidity of the cornea [4]. Mean value of ΔCRF was negative and our regression analysis showed that the only influencing factor relevant to the change of CRF was the CCT (regression formula: $\Delta CRF = 6.072 - 0.013 \cdot CCT$). This indicated that a thicker cornea would potentially indicate a larger decline in total corneal resistance to deformation due to cataract surgery, resulting from the decrease of viscoelastic resistance of the cornea [56]. This result coincides with the results from published literature, which states that a thicker cornea might potentially lead to a smaller change in CRF after standard cataract surgery [19, 30, 46]. This is due to the fact that CRF was originally designed to maximize the correlation of CRF with CCT or to minimize the correlation of CRF with IOP, based on the manufacturer's large-scale clinical data analysis [30].

SAI is a measure of central corneal asymmetry, which is used to determine the optical performance of the anterior corneal surface [57]. This facilitates a prediction of spectacle-corrected visual acuity based on the corneal surface topography [13]. Derived from our regression results, a lower corneal surface asymmetry may potentially indicate a smaller decline in cornea compensated IOP due to cataract surgery. A small fluctuation in IOP due to surgery may indicate satisfactory eye stability.

ECC reflects the cell density in corneal endothelium. A specific density is required to support dehydration of corneal stroma and maintain the corneal clarity. These basic rules are supported by the results of our study, which showed that a sufficient endothelial cell count may potentially indicate smaller fluctuation in IOP after cataract surgery. From this finding, we confirm the literature results that the cornea compensated IOP may offer an attractive alternative to traditional IOP measurement including Goldmann applanation tonometry. This might be of particular relevance for the evaluation and management of patients with normal IOP, where corneal biomechanics appear to play the greatest role for validity of IOP measurement [14]. However, absolute values of ΔIOPg were bigger than that of ΔIOPcc and both of

these values were negative, which indicates that IOPcc is less dependent on, but not completely independent of, corneal biomechanical properties. Even if change in IOPg and IOPcc after one month of cataract surgery are determined to be statistically significant, they are not of significant clinical relevance. In contrast, changes of CRF and CH after the surgery as observed in our study, may be of high clinical relevance. We hypothesize that corneal biomechanical properties are not independent of the biometric characteristics. In other words, biomechanical properties are affected or influenced by biometric characteristics. To the best of our knowledge, this is the first study providing potential predictive biometric parameters for the change of biomechanical values due to cataract surgery [48].

In a study by Roberts et al. statistically significant differences between myopic and hyperopic eyes in all ocular biomechanical output parameters were discovered. These parameters derived from analysis of the dynamic bidirectional applanation device air pressure and IR signals after cross-referencing for age and CCT [44]. Greater Peak1 has been reported to be associated with a stiffer cornea, along with other signal parameters [38]. The hyperopic dataset had a significantly greater Peak 1 than Peak 2, indicating these eyes were stiffer than the myopic eyes. Other parameters that supported this conclusion, were FWHM 1 and FWHM 2. FWHM 1 and 2 are parameters to describe the width of the indentation delivered by ORA. It is obtained by measuring the distance between 2 points on the curve, at which the function reaches half its maximum value (**Figure 9**). Both, FWHM 1 and 2, were significantly wider in the hyperopic eyes, indicating slower movement due to a stiffer cornea, which requires greater force to reach the same velocity. However, some parameters seemed to indicate the opposite relationship. Time 1 should be longer in stiffer eyes, since more force would be required to initiate motion as the air pressure increases in a stiffer eye. Yet, the hyperopic eyes had significantly shorter Time 1 than the myopic eyes. This seeming paradox was due to the significantly greater IOPcc in the myopic eyes, leading to longer Time 1. However, the result was reversed in the second comparison; Time 1 remained statistically significant, but controlling for IOPcc led to Time 1 being longer in hyperopic eyes, indicating greater stiffness.

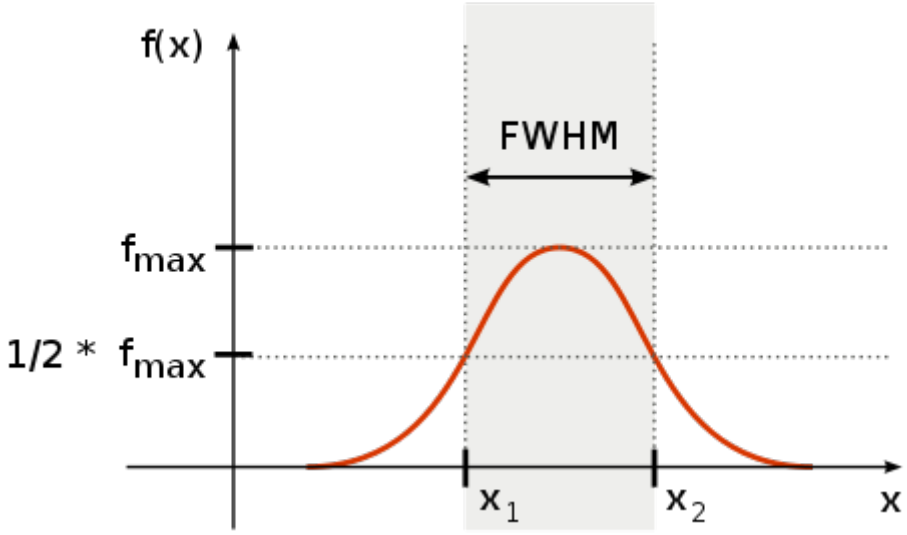

Fig 9: Area of full width at half maximum (red curve), FWHM 1 is defined as intersection of x1 on the curve, FWHM 2 is defined as intersection of x2 on the curve

Some studies have shown that CH may be independently linked to progressive glaucoma damage, suggesting that CH may be helpful for long-term monitoring of glaucoma and other diseases of the cornea, where intraocular pressure (IOP) plays a critical role, because it provides further information about the biomechanics of the cornea, beyond that of CCT [16].

Various hypotheses might explain the association between low CH and a larger magnitude of IOP reduction after cataract surgery. First, it is possible that cataract surgery lowers IOP evenly in eyes with low and high CH, but an eye with high CH might partially absorb the force applied by an instrument and prevent an accurate IOP reading, because most IOP measurements rely on corneal deformation and it is easier to measure IOP changes in eyes with low CH. This theory is consistent with previous studies that found a low pretreatment CH is associated with a greater magnitude of post treatment IOP reduction with different glaucoma therapies [2, 17]. A second possibility is that the association between low pretreatment CH and IOP reduction is mediated by high pretreatment IOP. Patients with low baseline CH often have a higher baseline IOP [2]. Because eyes with higher baseline IOP usually display a larger change in IOP after cataract surgery [10, 47], a high baseline IOP might be responsible for the association. A few considerations work against this possibility, however. This study was performed in patients without glaucoma; thus, the selection

criteria were not applied for patients with a high preoperative IOP. In addition, after multivariable regression analysis was performed to adjust for the baseline IOP, the baseline CH still independently contributed important information. Although a high baseline IOP might contribute to these results, it does not fully explain the association between CH and IOP reduction. A third possibility is that CH is simply a biomarker that randomly correlates with a structural or biomechanical feature of the eye that differentially affects individuals with low CH after cataract extraction. In summary, the use of a non-glaucomatous sample limits the application of this study. We believe that it allowed us to prove the concept that CH is associated with IOP reduction from cataract extraction. The present study further shows the potential uses of CH in clinical and research settings.

The roles of biometrical characteristics, endothelial cell count, and topography values on the change of biomechanical properties were discussed. ΔCH, ΔCRF, ΔIOPg, and ΔIOPcc decreased due to cataract surgery. If the predictive changes in biomechanics are validated in larger study populations, they should be considered in the routine values provided by the manufacturer of ORA. The limitation of this study was the small sample size and limited assessment parameters.

We are aware that our prediction was formulated with the linear regression analysis as a result of this pilot study and based on a limited number of populations. It has to be updated with a larger study population. However, the general concept of predictive changes of ORA values due to cataract surgery based on biomechanical measures is reasonable [48].

6. REFERENCES

1. Abahussin M, Hayes S, Knox Cartwright NE, Kamma-Lorger CS, Khan Y, Marshall J, Meek KM. 3D collagen orientation study in human cornea using X-ray diffraction and femtosecond laser technology. *Invest Ophthalmol Vis Sci* 2009;50:5159-64.

2. Agarwal DR, Ehrlich JR, Shimmyo M, Radcliffe NM. The relationship between corneal hysteresis and the magnitude of intraocular pressure reduction with topical prostaglandin therapy. *Br J Ophthalmol* 2012;96:254-257.

3. Akhtar S, Bron AJ, Salvi SM, Hawksworth NR, Tuft SJ, Meek KM. Ultrastructural analysis of collagen fibrils and proteoglycans in keratoconus. *Acta Ophthalmol* 2008;86:764–772.

4. Alió JL, Agdeppa MC, Rodríguez-Prats JL, Amparo F, Piñero DP. Factors influencing corneal biomechanical changes after microincision cataract surgery and standard coaxial phacoemulsification. *J Cataract Refract Surg* 2010;36:890–897.

5. Ascaso FJ, Huerva V (2013). The History of Cataract Surgery, Cataract Surgery, Dr. Farhan Zaidi (Ed.), ISBN: 978-953-51-0975-4, *InTech* DOI: 10.5772/19243. Available from: *http://www.intechopen.com/books/cataract-surgery/the-history-of-cataract-surgery.*

6. Benninghoff, Anatomie, Band 2, *Verlag Urban und Schwarzberg,* 1994, p.716.

7. Beuerman RW, Pedroza L. Ultrastructure of the human cornea. *Microsc Res Tech* 1996;33:320-35.

8. Boote C, Dennis S, Huang Y, Quantock AJ, Meek KM. Lamellar orientation in human cornea in relation to mechanical properties. *J Struct Biol* 2005;149:1-6.

9. Cho YK. Early intraocular pressure and anterior chamber depth changes after phacoemulsification and intraocular lens implantation in nonglaucomatous eyes. Comparison of groups stratified by axial length. *J Cataract Refract Surgery* 2008;34:1104–1109.

10. Congdon NG, Broman AT, Bandeen-Roche K, Grover D, Quigley HA. Central corneal thickness and corneal hysteresis associated with glaucoma damage. *Am J Ophthalmol* 2006;141:868-875.

11. Copeland RA, Afshari NA (Hrsg.) (2013). Copeland and Afshari's Principles and Practice of Cornea. 1st ed. Jaypee Brothers Medical Publishers, 2013, p.26-43.

12. Daxer A, Misof K, Grabner B, Ettl A, Fratzl P. Collagen fibrils in the human corneal stroma: structure and aging. *Invest Ophthalmol Vis Sci* 1998;39:644–648.

13. Dingeldein SA, Klyce SD, Wilson SE. Quantitative descriptors of corneal shape derived from computer-assisted analysis of photokeratographs. *Refract Corneal Surg* 1989;5:372–378.

14. Ehrlich JR, Radcliffe NM, Shimmyo M. Goldmann applanation tonometry compared with corneal-compensated intraocular pressure in the evaluation of primary open-angle Glaucoma. *BMC Ophthalmol* 2012;12:52.

15. Grehn F Augenheilkunde, Springer Medizin Verlag, Heidelberg, 31. Auflage, 2012, p.109-143.

16. Hager A, Schroeder B, Sadeghi M, Grossherr M, Wiegand W. The influence of corneal hysteresis and corneal resistance factor on the measurement of intraocular pressure. *Ophthalmologe* 2007;104:484-489.

17. Hirneiß C, Sekura K, Brandlhuber U, Kampik A, Kernt M. Corneal biomechanics predict the outcome of selective laser trabeculoplasty in medically uncontrolled glaucoma. *Graefes Arch Clin Exp Ophthalmol* 2013;251:2383-2388.

18. Johnson RD, Nguyen MT, Lee N, Hamilton DR. Corneal biomechanical properties in normal, forme fruste keratoconus, and manifest keratoconus after statistical correction for potentially confounding factors. *Cornea* 2011;30:516–523.

19. Kamiya K, Hagishima M, Fujimura F, Shimizu K. Factors affecting corneal hysteresis in normal eyes. *Graefes Arch Clin Exp Ophthalmol* 2008;246:1491–1494.

20. Kasper T, Bühren J, Kohnen T: Visual performance of aspherical and spherical intraocular lenses: intraindividual comparison of visual acuity, contrast sensitivity, and higher-order aberrations. *J Cataract Refract Surg* 2006;32: 2022–9.

21. Kinoshita S, Adachi W, Sotozono C, Nishida K, Yokoi N, Quantock AJ, Okubo K. Characteristics of the ocular surface epithelium. *Prog Retin Eye Res* 2001;20:639–73.

22. Klyce S, Beuerman R. Structure and Function of the Cornea. In: Kaufman HE, Barron BA, McDonald MB (Hrsg.) *The Cornea*. Second Edition. Butterworth-Heinemann, Newton, USA.1998; p.3-26.

23. Knupp C, Pinali C, Lewis PN, Parfitt GJ, Young RD, Meek KM, Quantock AJ. The architecture of the cornea and structural basis of its transparency. *Adv Protein Chem Struct Biol* 2009;78:25-49.

24. Komai Y, Ushiki T. The three-dimensional organization of collagen fibrils in the human cornea and sclera. *Invest Ophthalmol Vis Sci* 1991;32:2244-58.

25. Krachmer JH, Mannis MJ, Holland EJ. Basic Science and Pathophysiologic Responses, Fundamentals of Cornea and External Disease. Mosby, St. Louis, 1997; p.3-19.

26. Kroll P, Grunz C, Straub W (Hrsg.) Augenärztliche Untersuchungsmethoden. 3rd ed. Thieme, Stuttgart, New York, 2007, p.179-200.

27. Kucumen RB, Yenerel NM, Gorgun E, Kulacoglu DN, Oncel B, Kohnen MC, Alimgil ML. Corneal biomechanical properties and intraocular pressure changes after phacoemulsification and intraocular lens implantation. *J Cataract Refract Surg* 2008;34:2096–2098.

28. Leonhardt H, Tillmann B, Töndury G, Zilles K. Rauber/Kopsch-Anatomie des Menschen. Georg Thieme Verlag, Stuttgart, 1987, p.533-38.

29. Lim L, Gazzard G, Chan YH, Fong A, Kotecha A, Sim EL, Tan D, Tong L, Saw SM. Cornea biomechanical characteristics and their correlates with refractive error in Singaporean children. *Invest Ophthalmol Vis Sci* 2008;49:3852–3857

30. Luce DA. Determining in vivo biomechanical properties of the cornea with an ocular response analyzer. *J Cataract Refract Surg* 2005;31:156–162.

31. Maeda N, Klyce SD, Smolek MK, Thompson HW. Automated keratoconus screening with corneal topography analysis. *Invest Ophthalmol Vis Sci* 1994;35:2749–2757.

32. Mamalis N: OVDs. viscosurgical, viscoelastic, and viscoadaptive. What does this mean? J Cataract Refract Surg 2002;28:1497–8.

33. Marshall GE, Konstas AG, Lee WR. Immunogold fine structural localization of extracellular matrix components in aged human cornea. I. Types I–IV collagen and laminin. Graefes Arch Clin Exp Ophthalmol 1991;229:157-63.

34. Meek KM, Tuft SJ, Huang Y, Gill PS, Hayes S, Newton RH, Bron AJ. Changes in collagen orientation and distribution in keratoconus corneas. *Invest Ophthalmol Vis Sci* 2005;46:1948–1956.

35. Meek KM, Boote C. The use of X-ray scattering techniques to quantify the orientation and distribution of collagen in the corneal stroma. Prog Retin Eye Res 2009;28:369-92.

36. Morishige N, Wahlert AJ, Kenney MC, Brown DJ, Kawamoto K, Chikama T, Nishida T, Jester JV. Second-harmonic imaging microscopy of normal human and keratoconus cornea. *Invest Ophthalmol Vis Sci* 2007;48:1087-94.

37. Müller-Vogt I. Hochpräzise dreidimensioinale Bestimmung optischer und biomechanischer Eigenschaften der menschlichen Hornhaut. http://www.ub.uni-heidelberg.de/archiv/1387, Zugang am 25.05.2015.

38. Qazi MA, Sanderson JP, Mahmoud AM, Yoon EY, Roberts CJ, Pepose JS. Postoperative changes in intraocular pressure and corneal biomechanical metrics Laser in situ keratomileusis versus laser-assisted subepithelial keratectomy. *J Cataract Refract Surg* 2009;35:1774-1788.

39. Reichert, Inc. Ocular Response Analyzer Software Version 3.0 User's Guide, 2010, p 26 – 30.

40. Reichert, Inc. Understand the Cornea, Understand the Pressure Corneal Biomechanics and Accurate IOP in one Simple Instrument. interne Kommunikation von Reichert.

41. Reim M, Augenheilkunde. Ferdinand Enke Verlag, Stuttgart, 1993, p.37-43.

42. Riaz Y, Mehta JS, Wormald R, Evans JR, Foster A, Ravilla T, Snellingen T: Surgical interventions for age-related cataract. Cochrane Database of Systematic Reviews 2006; Issue 4.: Art. No.: CD001323. DOI: 10.1002/14651858.CD001323.pub2.

43. Riederle F, Buchwald HJ, Preissinger C, Lang GK. Refraktive Gesichtspunkte moderner Katarakt-Chirurgie. *Klin Monbl Augenheilkd* 2006;223: 943–51.

44. Roberts CJ, Reinstein DZ, Archer TJ, Mahmoud AM, Gobbe M, Lee L. Comparison of ocular biomechanical response parameters in myopic and hyperopic eyes using dynamic bidirectional applanation analysis. J Cataract Refract Surg 2014;40:929-936.

45. Sachsenweger M. Augenheilkunde. Hippokrates Verlag, Stuttgart, 1994, p.130-131.

46. Shah S, Laiquzzaman M, Cunliffe I, Mantry S. The use of the Reichert ocular response analyser to establish the relationship between ocular hysteresis, corneal resistance factor and central corneal thickness in normal eyes. *Cont Lens Anterior Eye* 2006;29:257–262.

47. Shingleton BJ, Laul A, Nagao K, Wolff B, O'Donoghue M, Eagan E, Flattem N, Desai-Bartoli S. Effect of phacoemulsification on intraocular pressure in eyes with pseudoexfoliation: single-surgeon series. *J Cataract Refract Surg* 2008;34:1834-41.

48. Song X, Langenbucher A, Gatzioufas Z, Seitz B, El-Husseiny M. Effect of biometric characteristics on the change of biomechanical properties of the human cornea due to cataract surgery. *Biomed Res Int* 2014; 2014:628019.

49. Song XF, Langenbucher A, Gatzioufas Z, Seitz B, El-Husseiny M. Effect of biometric characteristics on biomechanical properties of the cornea in cataract patient. *Intl J Ophthalmol* 2016;9(6):854-857.

50. Spörl E, Terai N, Haustein M, Böhm AG, Raiskup-Wolf F, Pillunat LE. Biomechanical condition of the cornea as a new indicator for pathological and structural changes. *Ophthalmologe* 2009;106:512–520.

51. Terai N, Raiskup F, Haustein M, Pillunat LE, Spoerl E. Identification of biomechanical properties of the cornea: the ocular response analyzer. *Curr Eye Res* 2012;37:553–562.

52. Touboul D, Roberts C, Kérautret J, Garra C, Maurice-Tison S, Saubusse E, Colin J. Correlations between corneal hysteresis, intraocular pressure, and corneal central pachymetry. *J Cataract Refract Surg* 2008;34:616–622.

53. Volkmer C, Pham DT, Wollensak J: Minimizing astigmatism by controlled localization of cataract approach with the no stitch technique. A prospective study. *Klin Monbl Augenheilkd* 1996;209:100–4.

54. Wenzel M, Pham D, Scharrer A, Schayan K, Klasen J (2008) Derzeitiger Stand der ambulanten Intraokularchirurgie: Ergebnisse der Umfrage 2007 des BDOC, BVA und der DGII. Ophthalmo-Chirurgie 20:137-146.

55. Wilson SE, Klyce SD. Quantitative descriptors of corneal topography. A clinical study. *Arch Ophthalmol* 1991;109:349–353.

56. Wilson SE, Hong JW. Bowman's layer structure and function: critical or dispensable to corneal function? A hypothesis. Cornea 2000;19:417-20.

57. WHO. World Health Organization (2004) Magnitude and causes of visual impairment. WHO. World Health Organization http://www.who.int/mediacentre/factsheets/fs282/en/

7. PUBLICATIONS AND CONFERENCE PARTICIPATIONS

Scientific publications:

1. Walter HS, Gatzioufas Z, El-Husseiny M, Stavridis E, Seitz B. Does intravitreal injection of ranibizumab increase the risk for macular hole formation. *Eur J Ophthalmol* 2011;21:680-681.

2. Gatzioufas Z, Hager T, El-Husseiny M, Kozeis N, Seitz B. Salzmann's nodular degeneration on a corneal graft 20 years after penetrating keratoplasty for keratoconus. *Ophthalmologe* 2011;108:963-965.

3. Gatzioufas Z, Huchzermeyer Cr, Hasenfus A, El-Husseiny M, Seitz B. Histological and biochemical findings in membranous cataract. *Ophthalmic Res* 2012;47:146-149.

4. Szentmáry N, Goebels S, El-Husseiny M, Langenbucher A, Seitz B. Immune reactions following excimer laser and femtosecond laser-assisted penetrating keratoplasty. *Klin Monbl Augenheilkd* 2013;230:486-489.

5. Seitz B, El-Husseiny M, Langenbucher A, Szentmáry N. Prophylaxis and management of complications in penetrating keratoplasty. *Ophthalmologe* 2013;110:605-613.

6. Seitz B, Cursiefen C, El-Husseiny M, Viestenz A, Langenbucher A, Szentmáry N. DALK and penetrating laser keratoplasty for advanced keratoconus. *Ophthalmologe* 2013;110:839-848.

7. El-Husseiny M, Tsintarakis T, Eppig T, Langenbucher A, Seitz B. Intracorneal ring segments in keratoconus. *Ophthalmologe* 2013;110:823-829.

8. Song X, Langenbucher A, Gatzioufas Z, Seitz B, El-Husseiny M. Effect of biometric characteristics on the change of biomechanical properties of the human cornea due to cataract surgery. *Biomed Res Int* 2014; 2014:628019.

9. Fiorentzis M, Viestenz A, El-Husseiny M, Szentmáry N, Seitz B. Subjective asymptomatic corneal opacity after Descemet membrane endothelial keratoplasty. *Ophthalmologe* 2015;112:276-278.

10. Tsintarakis T, Eppig T, Langenbucher A, Seitz B, El-Husseiny M. Can the implantable collamer lens with Aquaport technology safely prevent an angle block? Early experiences in the Homburg/Saar refractive surgery center. *Ophthalmologe* 2015;112:418-23.

11. Resch MD, Zemova E, Marsovszky L, Szentmáry N, Bauer F, Daas L, Pattmöller M, El-Husseiny M, Németh J, Nagy Zz, Seitz B. In Vivo Confocal Microscopic Imaging of the Cornea After Femtosecond and Excimer Laser-assisted Penetrating Keratoplasty. *J Refract Surg* 2015;31:620-626.

12. El-Husseiny M, Seitz B, Langenbucher A, Akhmedova E, Szentmary N, Hager T, Tsintarakis T, Janunts E. Excimer versus Femtosecond Laser Assisted Penetrating Keratoplasty in Keratoconus and Fuchs Dystrophy: Intraoperative Pitfalls.
J Ophthalmol 2015;2015:645830.

13. Eppig T, Spira C, Tsintarakis T, El-Husseiny M, Cayless A, Müller M, Seitz B, Langenbucher A. Ghost-image analysis in phakic intraocular lenses with central hole as a potential cause of dysphotopsia. *J Cataract Refract Surg* 2015;41:2552-2559.

14. Flockerzi E, El-Husseiny M, Löw U, Daas L, Seitz B. Cataract development after electrical injury. *Ophthalmologe* 2016 Mar 31. (Epub ahead of print) PMID: 27033227

15. El-Husseiny M, Daas L, Langenbucher A, Seitz B. Intracorneal Ring Segments to Treat Keratectasia – Interim Results and Potential Complications. *Klin Monbl Augenheilkd* 2016;233:722-726.

16. Seitz B, Szentmáry N, Langenbucher A, Hager T, Viestenz A, Janunts E, El-Husseiny M. PKP for Keratoconus – From Hand/Motor Trephine to Excimer Laser and Back to Femtosecond Laser. *Klin Monbl Augenheilkd* 2016;233:727-736.

17. Song XF, Langenbucher A, Gatzioufas Z, Seitz B, El-Husseiny M. Effect of biometric characteristics on biomechanical properties of the cornea in cataract patient. *Intl J Ophthalmol* 2016;9(6):854-857.

Scientific presentations:

1. El-Husseiny M. Femtosekundenlaser-Kataraktchirurgie - Implikation für refraktive IOL´s und I-Lasik in Homburg. 68. Homburger Augenärztliche Fortbildung HAF Homburg/Saar, Germany, 16.03.2011

2. El-Husseiny M & Seitz B. Laser in situ Keratomileusis (LASIK) after penetrating keratoplasty. 109. Kongress der Deutschen Ophthalmologischen Gesellschaft (DOG), Berlin, Germany, 29.09-02.10.2011

3. El-Husseiny M. Femtosecond laser Intrastromal Corneal Ring Segments (ICRS) implantation for the management of iatrogenic keratectasia after LASIK. 84. Versammlung der Vereinigung Rhein-Mainischer Augenärzte, Marburg, Germany, 05.11.2011

4. El-Husseiny M. Refractive surgery and keratoconus - topographic considerations. 1. Homburger Keratoconus Symposium im Rahmen der Homburger Herbstakademie, Homburg/Saar, Germany, 12.11.2011

5. El-Husseiny M. Femtosecond implantable corneal ring segments for post LASIK keratectasia. 1. Homburger Keratoconus Symposium im Rahmen der Homburger Herbstakademie, Homburg/Saar, Germany, 12.11.2011

6. El-Husseiny M. Femtosecond laser Intrastromal Corneal Ring Segments (ICRS) for the treatment of iatrogenic keratectasia after LASIK. XVIII. Ophthalmologische Optische Fortbildung, Münster, Germany, 15.01.2012

7. El-Husseiny M & Moussa S. Refraktive Chirurgie nach Keratoplastik. 2. Homburger Hornhauttag, Homburg/Saar, Germany, 02.06.2012

8. El-Husseiny M. Multifokale IOL – Was tun, wenn das Ziel verfehlt wurde? 72. Homburger Augenärztliche Fortbildung HAF, Homburg/Saar, Germany, 12.09.2012

9. El-Husseiny M. INTACS bei Keratoconus und iatrogener Keratektasie nach LASIK. 110. Kongress der Deutschen Ophthalmologischen Gesellschaft (DOG), Berlin, Germany, 20.-23.09.2012

10. El-Husseiny M, Tsintarakis T, Pattmoeller M. Gibt es verantwortungsvolle refraktive Chirurgie bei Myopia magna? ICL. 73. Homburger Augenärztliche Fortbildung (HAF), Homburg/Saar, Germany, 13.03.2013

11. El-Husseiny M, Tsintarakis T, Pattmoeller M. INTACS bei Keratoconus. 73. Homburger Augenärztliche Fortbildung (HAF), Homburg/Saar, Germany, 13.03.2013

12. El-Husseiny M & Tsintarakis T. INTACS bei Keratokonus und iatrogener Keratektasie nach LASIK. Münster Hornhaut Forum 2013, Münster, Germany, 27.04.2013

13. El-Husseiny M. Refraktive Chirurgie – Scharf Sehen ohne Hilfsmittel. Gesundheitsmesse, Blieskastel, Germany, 11.05.2013

14. El-Husseiny M & Seitz B. Wenn Scheinwerfer blenden oder der Durchblick getrübt ist - Eine Operation hilft gegen den Grauen Star. Gesundheitsmesse, Blieskastel, Germany, 12.05.2013

15. El-Husseiny M & Tsintarakis T. Intracorneale Ringe zur Behandlung des Keratokonus - Indikationen und Grenzen. 15. Ophthalmo-chirurgischer Nachmitag der ARTEMIS Augen- und Laserklinik, Frankfurt, Germany, 11.09.2013

16. El-Husseiny M, Tsintarakis T, Eppig T, Langenbucher A, Seitz B. INTACS bei Keratoconus. Ophthalmo-chirurgische Videos interaktiv: Kornea**.** 111. Kongress der Deutschen Ophthalmologischen Gesellschaft (DOG), Berlin, Germany, 19.-22.09.2013

17. El-Husseiny M, Szentmary N, Eppig T, Langenbucher A. OP-Besonderheiten, Implantation Kurs: Torische Intraokularlinsen – Von der Vorbereitung bis zur Nachsorge 111. Kongress der Deutschen Ophthalmologischen Gesellschaft (DOG), Berlin, Germany, 19.-22.09.2013 (Course Instructor)

18. El-Husseiny M & Tsintarakis T. LASIK & KAMRA-Inlay zur Behandlung von Fehl- & Alterssichtigkeit. 74. Homburger Augenärztliche Fortbildung (HAF), Homburg/Saar, Germany, 16.10.2013

19. El-Husseiny M, Janunts E, Langenbucher A, Akhmedova E, Tsintarakis T, Seitz B. Excimer- vs. Femtosekundenlaser gestützte Keratoplastik bei Keratokonus und Fuchs-Dystrophie – Intra- und frühpostoperative Ergebnisse einer prospektiven randomisierten Studie. 86. Versammlung der Vereinigung Rhein-Mainischer Augenärzte, Giessen, Germany, 2.11.2013

20. El-Husseiny M, Tsintarakis T, Seitz B. Das KAMRA-Inlay zur Presbyopiekorrektur – Prospektives Studiendesign und erste klinische Ergebnisse. 86. Versammlung der Vereinigung Rhein-Mainischer Augenärzte, Giessen, Germany, 2.11.2013

21. El-Husseiny M, Tsintarakis T, Eppig T, Langenbucher A, Seitz B. INTACS bei Keratoconus – Update. 3. Homburger Herbstakademie, Homburg, Germany, 09.11.2013

22. El-Husseiny M. Refraktive Chirurgie – Scharf Sehen ohne Hilfsmittel. Gesundheitsmesse, Dillingen, Germany, 22.03.2014

23. Viestenz Ar, El-Husseiny M, Seitz B. Management of CNV after globe perforation. 11. Congress of the International Society of Ocular Trauma, Dubrovnik, Croatia, 22.-25.05.2014 (Co-Author)

24. El-Husseiny M, Tsintarakis T, Langenbucher A, Seitz B. Intracorneal Ring Segments (ICRS) for Mid-Stage Keratoconus. World Ophthalmology Congress of the International Council of Ophthalmology (WOC), Tokyo, Japan, 02.-06.04.2014 (Invited Speaker)

25. El-Husseiny M. KAMRA Inlay. Lange Nacht der Wissenschaften (Saarland University Hospitals), Homburg/Saar, Germany, 06.06.14

26. El-Husseiny M. Korneales KAMRA-Inlay bei Presbyopie. 3. Homburger Hornhauttag, Homburg/Saar, Germany, 28.06.2014

27. El-Husseiny M. Intrastromale Ringe bei Keratokonus. Freiburger Kontaktlinsentag (Freiburg University Hospitals), Freiburg, Germany, 19.07.14 (Invited Speaker)

28. El-Husseiny M, Tsintarakis T, Langenbucher A, Seitz B. Komplikationen bei intracornealen Implantaten. 112. Kongress der Deutschen Ophthalmologischen Gesellschaft (DOG), Leipzig, Germany, 25.-28.09.2014 (Invited Speaker)

29. El-Husseiny M, Tsintarakis T, Seitz B. Das KAMRA-Inlay - ein realistischer Ansatz? Presbyopie-Symposium. 112. Kongress der Deutschen Ophthalmologischen Gesellschaft (DOG), Leipzig, Germany, 25.-28.09.2014 (Invited Speaker)

30. Seitz B, Janunts E, Langenbucher A, El-Husseiny M. Excimer versus Femtokeratoplastik – Status und Ausblick. 112. Kongress der Deutschen Ophthalmologischen Gesellschaft (DOG), Leipzig, Germany, 25.-28.09.2014 (Co-Author)

31. Seitz B, Janunts E, Langenbucher A, Szentmáry N, El-Husseiny M. Excimer vs femtosecond laser for non-mechanical keratoplasty – Where are the true benefits? EVER Symposium: Corneal Dystrophy & Laser Keratoplasty: Updates. Nice, France, 01.-04.10.2014 (Co-Author)

32. El-Husseiny M. KAMRA-Inlay und LASIK gegen Fehl- und Alterssichtigkeit. Woche des Sehens (Universitätsklinikum des Saarlandes), Homburg/Saar, Germany, 15.10.2014

33. Viestenz Ar, El-Husseiny M, Seitz B. Therapie der choroidalen Neovaskularisation nach Bulbusperforation. 87. Versammlung des Vereins Rhein-Mainischer Augenärzte, Frankfurt am Main, Germany, 08.11.14 (Co-Author)

34. Seitz B & El-Husseiny M. DMEK, KAMRA, INTACS – Neues aus der Hornhaut-Chirurgie. Augenärztlicher Qualitätszirkel, Trier, Germany, 12.11.14 (Co-Author)

35. El-Husseiny M, Daas L, Eppig T, Langenbucher A, Seitz B. Intrakornealen Ringsegmente (INTACS) bei Keratokonus, Post-LASIK-Keratektasie, pelluzider marginaler Degeneration und Z.n. Ferrara-Ring-Explantation. 29. Kongress der Deutschsprachigen Gesellschaft für Intraokularlinsen-Implantation, interventionelle und refraktive Chirurgie (DGII), Karlsruhe, Germany, 27.-28.02.2015

36. El-Husseiny M, Daas L, Eppig T, Langenbucher A, Seitz B. Korneales KAMRA-Inlay bei Presbyopie. 29. Kongress der Deutschsprachigen Gesellschaft für Intraokularlinsen-Implantation, interventionelle und refraktive Chirurgie (DGII), Karlsruhe, Germany, 27.-28.02.2015

37. Daas L, Langenbucher A, Seitz B, El-Husseiny M. Implantierbare Collamer-Linse (ICL) zur Korrektur hoher Ametropie. 29. Kongress der Deutschsprachigen Gesellschaft für Intraokularlinsen-Implantation, interventionelle und refraktive Chirurgie (DGII), Karlsruhe, Germany, 27.-28.02.2015 (Co-Author)

38. El-Husseiny M. Excimerlaser-assistierte DALK mit dem Schwind-Amaris. 77. Homburger Augenärztliche Fortbildung (HAF), Homburg/Saar, Germany, 04.03.2015

39. El-Husseiny M. KAMRA-INLAY - Presbyopiekorrektur mit Fernvisuserhalt. 77. Homburger Augenärztliche Fortbildung (HAF), Homburg/Saar, Germany, 04.03.2015

40. Daas L, Seitz B, El-Husseiny M. Fs-Laser-assistierte ICRS-Implantation bei Keratokonus, Post-LASIK Keratektasie und pelluzider marginaler Degeneration. 77. Homburger Augenärztliche Fortbildung (HAF), Homburg/Saar, Germany, 04.03.2015 (Co-Author)

41. Seitz B & El-Husseiny M. Wertvolle Tipps für DMEK aus der täglichen Praxis. 77. Homburger Augenärztliche Fortbildung (HAF), Homburg/Saar, Germany, 04.03.2015 (Co-Author)

42. El-Husseiny M, Daas L, Langenbucher A, Seitz B. Intracorneal rings for the management of keratoconus, post-LASIK ectasia and pellucid marginal degeneration. 1st International Egypt & Middle East Femtosecond Laser Eye Surgeries Congress, Cairo, Egypt, 21.-22.05.2015

43. El-Husseiny M, Daas L, Langenbucher A, Seitz B. Efficacy of the KAMRA corneal inlay for presbyopia correction in both phakic and pseudophakic patients. 1st International Egypt & Middle East Femtosecond Laser Eye Surgeries Congress, Cairo, Egypt, 21.-22.05.2015

44. El-Husseiny M. Korneale Lochblende zur Behandlung der Presbyopie - Das KAMRA-Inlay. 28. Internationaler Kongress der Deutschen Ophthalmochirurgen (DOC), Leipzig, Germany, 11.-13.06.2015 (Invited Speaker)

45. El-Husseiny M, Daas L, Langenbucher A, Seitz B. Efficacy of the KAMRA corneal Inlay for presbyopia correction in both phakic and pseudophakic patients. XXXIII. Congress of the European Society of Cataract & Refractive Surgery (ESCRS), Barcelona, Spain, 05.-09.09.2015

46. El-Husseiny M. Intacs for keratoconus - long-term results and potential complications. Advanced diagnosis and state-of-the-art therapeutic options of keratoconus. 3rd joint symposium of the Sektion Kornea of the German Ophthalmology Society (DOG) and the American Cornea Society. 113. Kongress der Deutschen Ophthalmologischen Gesellschaft (DOG), Berlin, Germany, 01-04.10.2015 (Invited Speaker)

47. Daas L, Seitz B, El-Husseiny M. Intraoperative Mikroperforation der Descemet-Membran bei Excimerlaser-gestützter DALK. Vorderabschnittsfallkonferenz. 113. Kongress der Deutschen Ophthalmologischen Gesellschaft (DOG), Berlin, Germany, 01-04.10.2015 (Co-Author)

48. Tsintarakis T, Eppig A, Langenbucher A, Seitz B, El-Husseiny M. Einfluss geometrischer Parameter auf den Effekt der Femtosekundenlaser-assistierten INTACS SK-Implantation bei kornealen Ektasien. 88. Versammlung des Vereins Rhein-Mainischer Augenärzte, Mainz, Germany, 07.11.2015 (Co-Author)

49. El-Husseiny M. Intacs und DALK bei Keratokonus. Homburger Cornea Curriculum, Homburg, Germany, 18.-21.11.2015

50. El-Husseiny M. Refraktive Chirurgie (LASIK, KAMRA) und Komplikations-management. Homburger Cornea Curriculum, Homburg, Germany, 18.-21.11.2015

51. El-Husseiny M. DMEK Wetlab Course. Homburger Cornea Curriculum, Homburg, Germany, 18.-21.11.2015 (Course Instructor)

52. El-Husseiny M, Daas L, Bischoff-Jung M, Pattmöller M, Seitz B. Moderne Refractive Chirurgie Fortbildung für Luxembourg Augenärzten, Luxembourg, 13.01.2016

53. El-Husseiny M, Daas L, Langenbucher A, Seitz B. Langzeitergebnisse nach KAMRA-Inlay-Implantation bei phaken und pseudophaken Patienten. 30. Kongress der Deutschsprachigen Gesellschaft für Intraocularlinsen-Implantation, interventionelle und refraktive Chirurgie (DGII), Mannheim, Germany, 11.-13.02.2016

54. Daas L, Langenbucher A, Seitz B, El-Husseiny M. Intrakorneale Ringsegmente (ICRS) zur Stabilisierung von Keratektasien. 30. Kongress der Deutschsprachigen Gesellschaft für Intraocularlinsen-Implantation, interventionelle und refraktive Chirurgie (DGII), Mannheim, Germany, 11.-13.02.2016 (Co-Author)

55. Viestenz An, Steinmetz P, El-Husseiny M, Seitz B, Viestenz Ar. Die Okuläre Pulsation wird durch Okulopression nach Retrobulbäranästhesie gesenkt. 30. Kongress der Deutschsprachigen Gesellschaft für Intraocularlinsen-Implantation, interventionelle und refraktive Chirurgie (DGII), Mannheim, Germany, 11.-13.02.2016 (Co-Author)

56. Seitz B & El-Husseiny M. Lamellar Keratoplasty (DMEK / Excimer-DALK) in Homburg. 79. Homburger Augenärztliche Fortbildung (HAF), Homburg, Germany, 02.03.2016

57. El-Husseiny M. 29. Internationaler Kongress der Deutschen Ophthalmochirurgen (DOC), Joint session with the International Society of Refractive Surgery (ISRS) of the American Academy of Ophthalmology (AAO), Session 4: Refractive Surgery on Trial.
Judge: Thomas Neuhann
Case 1: Corneal Inlays
Pro: Günther Grabner, Detlev R.H. Breyer, Moatasem El-Husseiny
Contra: Joern S. Joergensen, Edi Haefliger, Mike P. Holzer
Nürnberg, Germany, 09.-11.06.2016 (Invited Speaker)

Scientific posters:

1. Gatzioufas Z, Wennemuth G, Schirra F, El-Husseiny M, Seitz B. Gap junctional activity and Connexin 43 mapping in keratoconus. 109. Kongress der Deutschen Ophthalmologischen Gesellschaft (DOG), Berlin, 29.09.-02.10.2011

2. Tsintarakis T, Seitz B, El-Husseiny M. Implantierbare Collamer Linse (ICL) bei Myopia magna und hoher Hyperopie. 111. Kongress der Deutschen Ophthalmologischen Gesellschaft (DOG), Berlin, 19.-22.09.2013

3. Seitz B, Janunts E, Langenbucher A, Akhmedova E, Tsintarakis T, El-Husseiny M. Excimer vs. Femtosecond Laser Assisted Penetrating Keratoplasty in Keratoconus and Fuchs Dystrophy – Design and Intraoperative Results of a Prospective Randomized Study. 111. Kongress der Deutschen Ophthalmologischen Gesellschaft (DOG), Berlin, 19.-22.09.2013

4. Zemova E, Bauer FM, Daas L, Pattmöller M, Marsovszky L, Szentmáry N, El-Husseiny M, Seitz B, Resch M. Konfokale Biomikroskopie der Hornhaut nach perforierender Femtosekunden- und Excimerlaser-Keratoplastik bei Keratokonus und Fuchs-Hornhautdystrophie. 112. Kongress der Deutschen Ophthalmologischen Gesellschaft (DOG), Leipzig, 25.-28.09.2014

5. Daas L, Seitz B, Langenbucher A, El-Husseiny M. Efficacy of intracorneal ring segments for the management of keratoconus, post-LASIK ectasia and pellucid marginal degeneration. XXXIII. Congress of the European Society of Cataract & Refractive Surgery (ESCRS), Barcelona, Spain, 05.-09.09.2015

6. El-Husseiny M, Daas L, Langenbucher A, Seitz B. Das KAMRA-Inlay zur Presbyopiekorrektur bei phaken und pseudophaken Patienten. 113. Kongress der Deutschen Ophthalmologischen Gesellschaft (DOG), Berlin, Germany, 01-04.10.2015

7. Seitz B, Janunts E, Hager T, Langenbucher A, Akhmedova A, Szentmary N, El-Husseiny M. Astigmatismus und Visus nach Excimer- vs. Femtosekundenlaser gestützer perforierender Keratoplastic bei Keratokonus und Fuchs-Dystrophie. 113. Kongress der Deutschen Ophthalmologischen Gesellschaft (DOG), Berlin, Germany, 01-04.10.2015

8. ACKNOWLEDGMENTS

No one said it would be easy, but the guidance of a number of colleagues and staff has been invaluable in the progress of this work.

First and foremost, one person was there from the first day, **Professor Dr. Berthold Seitz** the Director of the Ophthalmology Department, Saarland University. He is my main supervisor and has been the most influential person throughout the last 4 years. **Professor Seitz** has provided the most enthusiastic and supportive guidance possible over the past years. He has helped me at every stage of the journey from the initial intent to undergo a dissertation to this final stage of submission. I have learned a lot from him and for this I will always have the greatest admiration and gratitude. Thank you, Professor Seitz, for your invaluable supervision and advice throughout this dissertation.

I am truly impressed of **PD Dr. Zisis Gatzioufas's** scientific competence, life experience and good will in my fruitful discussions with him. He is my co-supervisor and actually he was the one that initiated the idea of this dissertation.

I also wish to express my gratitude to **Professor Achim Langenbucher**, the Head of the Experimental Ophthalmology Department. He introduced me to the fascinating field of experimental ophthalmology and statistics and not to mention the enormous amount of work he has done for this dissertation regarding the data banks, methods and statistical advice.

I would like to thank **Dr. Xuefei Song** for his support during the phase of data collection and for performing many of the patients' postoperative examinations.

I extend my profound gratitude to **Dr. Tobias Hager** for his unequivocal support and guidance. He made my journey throughout the writing up phase of this dissertation less bumpy. I have great respect to **Dr. Hager** for what he knows and can.

I would like to express my appreciation to **Mrs. Indrite Backes** for helping to schedule examination appointments with the patients and her constructive support to Dr. Song both with the investigating machines and language difficulties. At the same

time, I am very thankful to all the **patients** who willingly took part in, and supported this study.

I have been lucky to have embarked on this dissertation alongside many **great colleagues**, whom I would like to express my appreciation for their friendship, support, motivation and for making the journey rewarding and exciting. A special thank you to all my colleagues and hospital staff.

Finally, and more notably, I would like to thank my parents, Mohsen and Rawya, my son, Mohannad, my siblings, Moataz, Momen and Mennat, as well as the rest of my family. A dissertation has its highs and lows, a rollercoaster of failure and triumph, throughout which my family stood by me. Their love and unconditional support holds the responsibility for developing the person I am today, and I dedicate this dissertation to all of them.